Water Quality Monitoring in Freshwater Bodies with High-Density Spatial Mapping

By

Michael W. Saminsky

Department of Bioresource Engineering

Faculty of Agricultural and Environmental Sciences

McGill University, Montreal

December 2015

A thesis submitted in partial fulfillment of the requirements of

the degree of Master of Science

© Michael W. Saminsky, 2015

Abstract

In response to concerns of eutrophication and nutrient pollution in freshwater, there has been growing interest in how best to monitor the changing dynamics of water quality constituents. The objective of this study was to develop a monitoring technique effective both in identifying nutrient loading sites and quantifying spatiotemporal changes of critical water quality indicators in two shallow ponds which experience duckweed (Lemna sp.) blooming in response to eutrophic conditions. From May to July 2014, weekly monitoring at 12 control locations of dissolved oxygen (DO), temperature (T), pH, as well as inorganic and organic forms of nitrogen (N) and phosphorus (P) was pursued to characterize temporal dynamics influenced by the drainage of nearby agricultural fields as well as by the duckweed bloom. Two high-density (<3 m) spatial sensing events in June and August of DO, NO_3^--N, T, and pH, were completed to characterize spatial dynamics and identify the placement of temporal sampling locations. Weekly monitoring revealed that dissolved N and particulate P concentrations were slightly higher near subsurface drain inflow locations than within the body of the ponds, and that duckweed blooms rapidly depleted dissolved oxygen to below 1.0 mg L^{-1}, depleted NO_3^--N, lowered but stabilized pH levels at a pH of 7.0, and inhibited nitrification by creating anoxic conditions. High-density mapping revealed that DO, NO_3^--N, and T exhibited reduced spatial structure after duckweed blooms. Additionally, mapping of DO, pH, and NO_3^--N was used to identify nutrient loading sites. It is beneficial to select sampling locations for continuous temporal monitoring based on water quality maps. This mapping should take place after snowmelt and before biological activity causes regime shifts that reduce the spatial structure of water quality constituents.

Résumé

En réponse aux préoccupations de l'eutrophisation de l'eau douce et de pollution par les nutriments dans l'eau douce, il y a un intérêt grandissant quant à la meilleure façon d'examiner la dynamique changeante des constituants de la qualité de l'eau. L'objectif de cette étude était de développer une technique de surveillance efficace à la fois dans l'identification des points chauds polluants et dans la quantification des changements spatio-temporels des indicateurs essentiels de la qualité de l'eau dans deux étangs peu profonds qui subissent des épisodes de prolifération de la lentille d'eau (genre Lemna) en réponse aux conditions d'eutrophisation. Un suivi hebdomadaire à 12 endroits de la teneur en oxygène dissous (TOD), de la température (T), du pH, ainsi que des formes organiques et inorganiques de l'azote (N) et du phosphore (P) a été conduit afin de caractériser la dynamique temporelle influencée par le drainage des champs agricoles à proximité ainsi que par la prolifération de la lentille d'eau. Deux événements de détection spatiale à haute densité (<3 m) des TOD, NO_3^--N, T, et du pH, ont été conduits en juin et en août pour caractériser les dynamiques spatiales et identifier l'emplacement de sites d'échantillonnage temporels. Un suivi hebdomadaire a révélé que les concentrations d'azote dissous et de phosphore particulaire étaient plus élevées à proximité des points d'évacuation de drainage que dans le reste des étangs, et que les épisodes de prolifération de la lentille d'eau épuisaient rapidement l'oxygène dissous au-dessous de 1,0 mg L^{-1}, réduisaient le NO_3^--N dissous, abaissaient, mais stabilisaient les niveaux de pH légèrement au-dessus du pH neutre, et empêchaient la nitrification en créant des conditions anoxiques. La cartographie de la qualité de l'eau à haute densité a révélé que la structure spatiale est réduite pour le TOD, NO_3^--N et T, En outre, la cartographie de TOD, pH, et NO_3^--N était utilisé pour identifier les sites des éléments nutritifs. Il est avantageux de sélectionner les sites d'échantillonnage pour le suivi temporel en se basant sur des cartes de qualité de l'eau. Cette cartographie doit être faite après la fonte des neiges et avant que l'activité biologique cause des changements de régime qui réduisent la structure spatiale de la qualité de l'eau.

On a summer morning
I sat down
on a hillside
to think about God -

a worthy pastime.
Near me, I saw
a single cricket;
it was moving the grains of a hillside

This way and that way.
How great was its energy.
How humble its effort.
Let us hope

it will always be like this.
Each of us going on
in our inexplicable ways
building the universe.

-Mary Oliver

To

the memory of

Issac Reznik

Acknowledgements

I would first like to express my sincere thanks to my supervisors Dr. Shiv Prasher & Dr. Viacheslav Adamchuk, for their guidance, support, and constant motivation. I would also like to thank Helene Lalande for her assistance with my laboratory work, and the continuing kindness she showed me. A special thanks to Kathy Zarayan from our own Soil and Water Quality Laboratory, who helped me set a course for success in my work. I thank Dr. Eman ElSayed for her friendship and guidance, and Dr. Abdul Mannan for his unceasing hard-work and willingness to impart his knowledge. Gratitude is also extended to Antoine Pouliot for translating, and to Dr. Ramanbhai Patel and Darline Canning who edited my thesis. I would also like to thank Dr. Timothy Schwinghammer, Dr. Pierre Dutilleul, Dr. Asim Biswas, Hsin-Hui Huang, Nandkishor Dhawale, Dr. Luan Pan for the technical and statistical help they provided.

I extend a deep thank you to my colleagues who helped me in the field, without whom I would still be collecting water samples in the ponds: Bharath Sudarsan, who battled snapping turtles at dawn by my side; Francisco Ruiz de la Macorra, whose positive attitude was of great moral support, and Rahul Suresh, whose infectious energy and drive made sampling go by much faster. I would also like to thank Florian Reumont, Martina Brun, Abu Mahdi Mia, Anisha Patel, and Daniela Vela who were instrumental to the success of this project.

The sincerest gratitude I can muster goes to my friends who supported me throughout this project and helped me better myself. Thank you to Bharath, for re-instilling in me a sense of curiosity about the world; Ann, who was never selfish with her gift of humour; Line, who taught me the words balance and break; Antonio, Paco, Dave, Nada, Tessie, Cecy, Daniela, Evan, and Yasmeen for their constant and unwavering support in the early mornings and late nights; and Marcela and Juanita, who provided their expert guidance in all matters of design. A special thank you to my four dear friends Spencer, Sam, Jack, and Ali who kept me accountable and helped motivate me to finish this project (despite my very best efforts to the contrary).

I cannot adequately express my gratitude for my parents and sister for their moral support, love, and encouragement.

Finally I would like to thank NSERC, which provided the financial support that made this study possible, and Vemco, which provided equipment for this study.

Table of contents

List of figures

List of tables

List of abbreviations and symbols

AUV	Autonomous Underwater Vehicle
DGE	Duckweed Growth Event
DO	Dissolved Oxygen
DON	Dissolved Organic Nitrogen
DOP	Dissolved Organic Phosphorus
DIN	Dissolved Inorganic Nitrogen
DIP	Dissolved Inorganic Phosphorus
DRP	Dissolved Reactive Phosphorus
DSP	Dissolved Soluble Phosphorus
ESC	Electronic Speed Control
IDW	Inverse-Distance Weighting
LP	Lower Pond
LS means	Least-Square means
MC	Microcontroller
Ortho-P	Ortho-Phosphate (PO_4^{3-})
PN	Particulate Nitrogen
PP	Particulate Phosphorus
QQ-plot	Quantile-Quantile plot
ROV	Remote-Operated Vehicle
T	Temperature
TAN	Total Ammonical Nitrogen
TDN	Total Dissolved Nitrogen
TDP	Total Dissolved Phosphorus
TN	Total Nitrogen
TP	Total Phosphorus
UP	Upper Pond
USV	Unmanned Surface Vehicle
UAV	Unmanned Aerial Vehicle
WHAT	Web-based Hydrographic Analysis Tool

1. Introduction

1.1. Problem statement

Agricultural runoff has been studied for decades, yet remains one of the most pervasive threats to freshwater systems and the services they provide humans and the environment: these include provisional services such as drinking water, supporting services such as nutrient cycling, primary production, and supporting biodiversity, regulating services such as water quality maintenance, flood and erosion control, and carbon sequestration, and cultural services such as recreational use, and spiritual and historical value (Aylward *et al.*, 2005). Though runoff contains a wide range of pollutants like nutrients (Carpenter *et al.* 1998), heavy metals (He *et al.*, 2003), antibiotics and pharmaceutically active compounds (Dolliver and Gupta, 2008; ElSayed *et al.*, 2013), pesticides and herbicides (Solomon *et al.*, 1996), and hormones (Ying, 2002), it is nutrients – largely in the form of nitrogen and phosphorus – that remain the principal determinants of freshwater ecosystem degradation (Han *et al.*, 2012; Jarvie *et al.*, 2013). Although the causes of ecosystem degradation are known, the effect – pollution - varies widely on spatial and temporal scales.

1.2. Justification

To improve our understanding of the sources and scale of pollution due to agricultural runoff, as well as to evaluate mitigation and management practices, there must be effective methods to monitor water quality in space and time (Hestir *et al.*, 2015). Different research and monitoring programs assess water quality on a wide range of spatiotemporal scales, depending on the scope and objective of the program. New technologies such as automated water samplers and *in-situ* sensors have allowed for higher resolution temporal studies, investigating annual, seasonal, intra-seasonal, weekly, diurnal, hourly, and even second-to-second trends in water (Bierman *et al.*,

2011; Smeltzer *et al.*, 2012). However, implicit assumptions of homogeneity, high costs of equipment and labor, and technological limitations have impeded high-resolution spatial studies of water quality (Casper *et al.*, 2012). New technologies such as remotely-operated and unmanned vehicles have created an opportunity to improve our understanding of nutrient and physicochemical property dynamics on the small scale (Garcia-Cordova, 2013; Hains and Kennedy, 2002; Raimondi *et al.*, 2015; Teece, 2009). Evaluation of such technologies is still needed.

1.3. Objectives

The ultimate goal of this research was to develop a spatiotemporal surface water monitoring strategy that would allow for the identification and quantification of polluting hotspots caused by nonpoint source agricultural pollution. The monitoring scheme was to combine temporal monitoring at a limited number of points with high spatial density mapping. The specific objectives were: 1) to assess spatiotemporal changes in water quality due to the blooming of a dense, floating, aquatic macrophyte, and 2) to determine if high-resolution water quality mapping can be used to identify nutrient loading sites in a small eutrophic pond.

1.4. Scope

This research was completed from May-August 2014 in two agricultural drainage ponds which received inflow from a combination of open-air ditches, subsurface drainage pipes, and surface runoff. Measured nutrient concentrations and activity were typically higher than the eutrophic trigger limits of 0.03 mg P L^{-1} of total phosphorus and 1.1 mg N L^{-1} of total nitrogen (Chambers *et al.*, 2012), but were also lower than the concentrations seen in heavily polluted agricultural freshwater systems.

1.5. Thesis format

Chapter two is a literature review synthesizing research on nutrient loading and eutrophication, spatiotemporal variability of nutrients and other critical freshwater parameters, and current monitoring techniques used in water quality monitoring. Chapter three describes the study site and field measurements of the research completed on pond nutrient dynamics between May-August 2014, followed by chapter four describing results and discussion. Chapter five describes a set of conclusions and recommendations of future work, and finally chapter six provides a list of the references used throughout the thesis. Chapter six is followed by the appendices that describe additional material including an overview of the design and testing of an Unmanned Surface Vehicle (USV) as a sensor platform. This USV was used to test a sensor platform and several innovative sensors being developed at McGill University.

2. Literature Review

2.1. Agricultural runoff – a global and local challenge

Human activities have had a drastic impact on the global cycling of nutrients, leading to a 108% increase in nitrogen, and a 400% increase in phosphorus being actively cycled (Bennett *et al.*, 2001; Falkowski, 2000). One of the major human activities responsible for this increase is agriculture and the diffuse runoff from pastures, managed grasslands, and other land uses associated with the agricultural industry (Rousseau *et al.*, 2013). The runoff is referred to as **nonpoint source (NPS) pollution** because it originates not from a single outflow or pipe, but from diffuse sources like surface runoff from land (Baker, 1992). Agricultural NPS runoff comprises organic and inorganic fertilizers containing ammonium, nitrate, and phosphate, and is symptomatic of intensive agricultural management practices and techniques that have become commonplace since their introduction in the 1950s after World War II (Novotny, 1999). Practices and phenomena like excess application of inorganic fertilizer (Liang and MacKenzie, 1994), land use conversion for agricultural purposes, soil erosion and soil loss from fields, as well as increased and intensive animal husbandry have all contributed to high nutrient loading in fresh water bodies (Peukert *et al.*, 2014).

2.1.1. Agricultural NPS pollution in Quebec

Across all of Canada's surface water, nearly 49% of N loading is attributed to agricultural runoff (Rasouli *et al.*, 2014). In Quebec, agricultural NPS pollution is one of the main factors for water quality degradation (Rousseau *et al.*, 2013). In 2011, the Ministry of Environment of Quebec (2011) placed freshwater nutrient management as a key objective for a 15 year conservation agreement between Quebec and federal institutions for managing the St. Lawrence River, a major freshwater resource in Eastern Canada. There is definite cause for concern about

freshwater quality in Quebec – in a 2007 study on the water quality status of Quebec lakes, 22 of 154 freshwater lakes were determined to be **eutrophic**, meaning that the water became enriched with growth-limiting nutrients like nitrogen and phosphorus, and would require immediate nutrient reduction management to see improvement (Galvez-Cloutier and Sanchez, 2007). Without proper intervention the number of nutrient-rich lakes will increase and water quality will further degrade - especially due to the risk-multiplying effects of climate change. Indeed, in 2014, volunteer monitoring as part of Quebec`s sustainable development, environmental, and climate change fighting initiative identified 45 lakes with algal blooms – a symptom of eutrophication (MDDELC, 2015).

2.2. Eutrophication

Eutrophication can affect both environmental and human health (Hudnell, 2010). When eutrophication occurs, photosynthetic algae, bacteria, and opportunistic aquatic vegetation that are all typically limited by a lack of nutrients have an opportunity for rapid growth – a phenomena referred to as blooming (Carpenter *et al.*, 1998). In freshwaters, the algal bloom is most typically due to cyanobacteria and blooming events are referred to as cyanobacterial toxin poisonings (CTP) or Harmful Algal Blooms (HABs) (Carmichael, 2001).

HABs deteriorate ecosystem health by inhibiting sunlight penetration, releasing harmful toxins, causing foul odors and tastes, and deoxygenating water (Paerl *et al.*, 2001). In the case of deoxygenation it is not the bloom that is the concern – but rather the algal and bacterial decay that follows a bloom. Algae and plankton are large controllers of oxygen and nutrient dynamics in ponds due to growth-decay cycles, and when massive algal bloom side off, the oxygen in the water is depleted as decomposing bacteria breakdown the organic matter (Yang *et al.*, 2008). Ultimately, this leads to large-scale biodiversity loss (Martinuzzi *et al.*, 2014) and loss of

ecosystem services like potable water, recreational capacities of water, and other (Carpenter *et al.*, 1998).

2.3. Fate of transported pollutants

Pollutants may be loaded into freshwater systems from agricultural fields and pastures by two mechanisms: 1) via surface transport through soil and surface erosion, and 2) via subsurface drainage systems, like tile drainage, that are typical for areas like Southern Quebec which experience high snowmelt and rainfall (Gollamudi *et al.*, 2007). Several factors determine the fate of the transported nutrient pollutants in freshwater – be they nitrogen or phosphorus – including source, concentration, bio-availability, form (inorganic or organic; dissolved or particulate), and the timing and location of load (Evans and Johnes, 2004; Stutter *et al.*, 2008). Once the pollutants have been loaded they can remain in the water column, interact with the sediment layer, and impact biological and physicochemical processes (House, 2003).

2.3.1. Fate of phosphorus in freshwater bodies

Phosphorus (P) is a relatively immobile nutrient, and it is typically sorbed in particulate form to soil and loaded into freshwater systems via agricultural surface runoff (Sims *et al.*, 1998), though it can be transported via tile drainage systems too (Beauchemin and Simard, 2000; Jamieson *et al.*, 2003). When it is in the form of particulate phosphorus (PP), P transport decreases as suspended particles tend to settle into the sediment in slow-moving water (Arheimer and Lidén, 2000). Phosphorous transport can be quicker when it is in the form of dissolved phosphorus, which is dissolved organic P (DOP) or dissolved inorganic phosphorus (DIP) – the latter is also referred to as soluble reactive P (SRP), dissolved reactive P (DRP), or orthophosphate (Ortho-P) (Yates, 2008). The phosphorus cycle is notoriously complex in aquatic systems and can be very dynamic due to the behavior of its various organic and inorganic fractions.

From the entire composition of P loaded into freshwater, the only immediately available form of P is the inorganic DRP which is immediately available for uptake by both macrophytes and algae to produce organic matter (Bostrom *et al.*, 1988a). As P is a limiting nutrient, it is rapidly taken up, and therefore freshwater concentration of DRP is often low (Reinhardt *et al.*, 2005).

Although PP and DOP are less immediately-available sources of P than DRP, these two fractions are important in P transport in agricultural runoff as agricultural P loads can be dominated by these two fractions (Stutter *et al.*, 2008). Both PP and DOP become bio-available through decomposition and mobilization driven by biogeochemical mechanisms in the water column and especially in the sediment layer (Bostrom *et al.*, 1988). In this way, the sediment becomes an important and delayed source of P (House, 2003).

The primary mechanism of sediment P release is the redox dissolution of ferric iron-phosphate that occurs under anaerobic, reducing conditions at the sediment-water interface (SWI). This mechanism was first described by Clifford Mortimer in a 1941 study illustrating that phosphates bound to insoluble ferric iron, more properly called iron (III) oxide. It would be released from the sediments of lakes as the SWI became anoxic and reducing, enabling iron (III) oxide to oxidize to ferrous iron – iron (II) oxide – and to release its bound phosphate. Another mechanism for P release from the sediments is the mineralization of sediment organic P pools, catalyzed by bacteria in the SWI (Gächter and Meyer, 1993). In this mechanism, bacteria convert organic P to orthophosphates, and under anoxic conditions rapidly decay and release DRP.

A review of P release from sediment completed by Hupfer and Lewandowski (2008) cast doubt on the importance of the oxygen-controlled dissolution of P bound to iron (III) oxide, highlighting research that pointed to $Al(OH)_3$ and unreducible iron (III) minerals that prevented

the P mobilization, even in anoxic conditions. The review concluded that there were other important mechanisms, like the dissolution of calcium-bound P or the anaerobic and aerobic decomposition of organic P. However, Amirbahman *et al.* (2013) showed that it was largely the iron (III) oxide-phosphate dissolution mechanism that drove these processes in both eutrophic and oligotrophic small, shallow lakes. In this study they neither discount the decomposition of organic P nor of other processes occurring above the sediments, and they found that P mineralization could occur above the SWI and within the water column itself, allowing for rapid P transformations within the water column from unavailable PP and DOP to bio-available DRP.

2.3.2. Fate of nitrogen in freshwater bodies

Nitrogen (N) is more mobile than P, and is often loaded from farmland into surface waters by runoff or subsurface flow. In Quebec and Ontario, nearly 50% of precipitation discharges as subsurface runoff through tile drainage systems (Simard, 2005) – carrying anywhere from 7.2 to 11.7 kg N ha^{-1} from the farmland (De Jong *et al.*, 2009). Runoff can comprise soluble inorganic $NO3^-$-N and ammonical N, particulate N (Rasouli *et al.*, 2014), and dissolved organic N (van Kessel *et al.*, 2009). The different fractions of N are variably available to biotic life, and their fates depend on seasonality and five nitrogen-cycling reactions: nitrification, denitrification, anaerobic ammonium oxidation (anammox), assimilation, and mineralization (Fig 2.1).

Loading introduces organic N and bio-available forms of dissolved N – like inorganic NO_3^--N and ammonical N - to freshwater systems. In water loaded from subsurface drainage ditches, even organic N can become biologically available via **mineralization,** a microbially mediated reaction (Skaggs *et al.*, 2005). Inorganic, bioavailable N can then be rapidly fixed into organic nitrogen compounds by primary producers through **assimilation –** a process that occurs rapidly when ecosystems are N-limited (Howarth al., 1988). Assimilation by primary producers typically

reduces dissolved inorganic N concentrations throughout the summer season (Heini *et al.*, 2014). Ammonical N that is not assimilated can be oxidized – under oxic conditions – to become NO_3^- by aerobic bacteria in the water column and oxic surface of the sediment layer in a two-step process, called **nitrification**. In eutrophic systems, these internal loads are a less significant source of NO_3^- than external loads (Johnes and Burt, 1993).

A relatively more significant reaction is **denitrification**, or the reduction of dissolved $NO_3^- \rightarrow N_2$ gas. N_2 gas is largely inert and is released through the water column and into the atmosphere (Rysgaard et al, 1994). Denitrification is performed by facultative anaerobic heterotrophic bacteria that typically reside in the anoxic zone of the sediment 5 cm beneath the surface, where low O_2, abundant NO_3^- available from nitrification, and a high availability of labile organic carbon creates an environment conducive to denitrification (Burgin *et al.*, 2012; Cornwell *et al.*, 1999). Denitrification by heterotrophs is not the only pathway of N loss from an aquatic system – **anammox**, or the anaerobic oxidation of ammonium converts $NO_2^- + NH_4^+ \rightarrow N_2 + 2H_2O$ and is performed by strictly anaerobic autotrophs (Kumar and Lin, 2010).

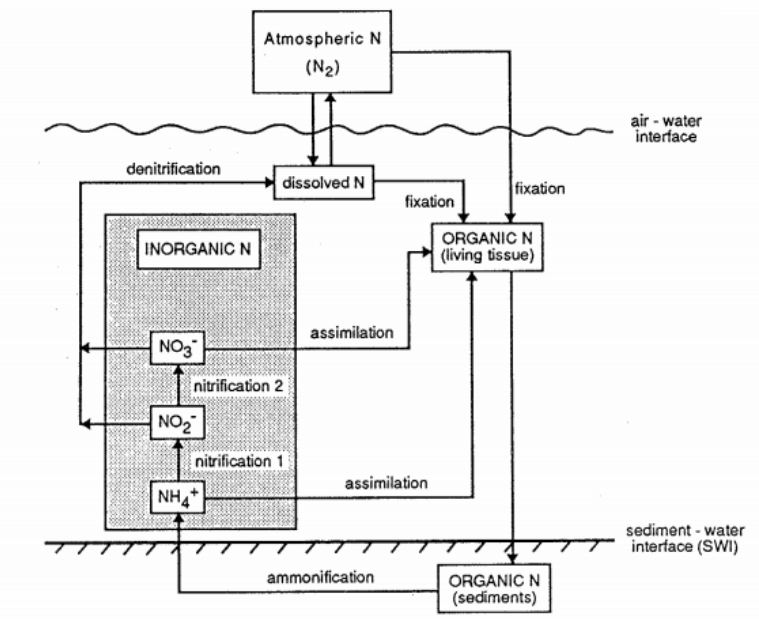

Fig. 2.1. The aquatic nitrogen cycle (Johnes and Burt, 1993).

2.4. Spatial and temporal variability of pollutants in water bodies

The fate of pollutants is largely dependent on complex dynamics both on land and in the water, causing significant variations in concentrations spatially and temporally. It is important to keep in mind scale in discussing spatiotemporal dynamics, as it can drastically change the type of outcomes and solutions that can be derived from studying water quality (Buck *et al.*, 2004; Casper *et al.*, 2012; Pratt and Chang, 2013; Vance-Borland *et al.*, 2008). Due to improvements in technology, researchers have been able to study high spatial and temporal resolution trends, which illustrated important interactions and diurnal cycles in HABs and pollutants (Huang *et al.*, 2014). The same has not been accomplished in the spatial dimension. Studies of freshwater spatiotemporal dynamics still tend to maximize the area sampled because of implicit assumptions of water homogeneity in space, as well as to make the best use of limited resources. A brief overview of spatiotemporal studies of water quality is presented below, to summarize the existing research completed and the scales that have been investigated. Due to the number of studies quantifying spatiotemporal trends in water quality – greater than 10,000 scientific articles according to a Web of Science citation search (Science Citation Index Expanded, 1899-2015) – this review is limited to recent studies investigating the annual, seasonal, and diurnal water quality trends of water receiving agricultural pollutant loads.

2.4.1. Catchment trends

Catchments – also known as drainage basins or watersheds – are the total area of land in which water on the surface and water stored beneath surface drains to a single water body or point (US EPA, 2012a). Catchment sizes can range from small, agricultural drainage basins of 0.05 km^2 to wide river drainage basins of 15,000 km^2 (Pilgrim *et al.*, 1982). Since catchments comprise both

terrestrial and aquatic components, studies often focus on the relationship between land-use and water quality.

It has been well-established that land-use has tremendous implications on water quality at the catchment scale. In a review of 35 catchments in an intensively agricultural area of Sweden, Arheimer and Lidén (2000) found that the amount of arable land was strongly correlated (*Kendall's $\tau = 0.61$; $p = 0.05$*) to the amount of bio-available inorganic nitrogen in the water. Correlations between agricultural land-use and nutrient loading have been seen in North America, too. In a four-year study conducted in North Dakota, concentrations of nitrate-nitrite and kjeldahl nitrogen (the sum of organic and ammonical nitrogen) were positively correlated with the number of animal feed operations in a drainage basin (Vandeberg *et al.*, 2015). In an analysis of 50 years of long-term monitoring data on Lake Champlain, Smeltzer *et al.* (2015) found that land-use conversion to higher phosphorus-yielding uses around Lake Champlain caused increases in total P across the last several decades.

Land-use effects can be dampened or multiplied based on varying hydrological characteristics of basins, like discharge. For the Lake Taihu Basin in eastern China, Li *et al.* (2014) found that discharge multiplied the effect of land-use on agricultural runoff – that 67-75% of nutrient loads to Lake Taihu came from three high-discharge areas of the basin. This was in line with other studies highlighting the effect of discharge and flow on nutrient load (Smeltzer *et al.*, 2012; Stutter *et al.*, 2008). However, discharge rates are not constant and can vary seasonally, especially in areas with notable wet and dry seasons. Moodley *et al.* (2015) investigated the relationship between land-use and nutrient runoff in three freshwater systems in South Africa during wet and dry seasons, and found that only during the wet season there were correlations between land-use and runoff.

Though a variety of temporal scales are assessed for catchment-scale studies, seasonal trends have been most useful for assessing the spatiotemporal dynamics in agricultural catchments, due in part to changes in discharge rates as mentioned earlier, and largely due to the seasonality of agricultural practices (Shrestha and Kazama, 2007). A review of NPS nitrogen export trends in Europe and North America by Causse *et al.* (2015) implicated variable fertilizer applications and crop rotations as determinants of the seasonal variability of catchment water quality. It is also at the seasonal temporal scale that HABs are often managed, though there is evidence to show that short-term onsets are better understood when diurnal patterns are investigated (Huang *et al.*, 2014).

2.4.2. Large water body trends

Within large bodies of water, there can be substantial spatiotemporal variability. Heini *et al.* (2014) investigated the relationship between phytoplankton and nutrients, pH, and oxygen in a large (103 km^2) eutrophic lake in Finland, and found that all measured parameters varied greatly in time and space. However, variability was not consistent and the greatest variability of N and P was during the onset of cyanobacterial blooms, when spatial structures were dynamic due to algae growth and uptake of nutrients, and spatial structures were undisturbed due to low wind and a microcystin layer of scum on the surface of the lake that prevented disturbances to the water below. They concluded that phytoplankton populations were impacting the spatial and temporal structures of water quality parameters in a measurable way within the lake.

Recently, a number of studies have reported on the dynamics of pollutants in the large, shallow Lake Taihu, as it is an important source of drinking water for much of China, and recent eutrophication events led to concerns over its water quality (Qin *et al.*, 2012). In a study published in 2014, Ye *et al.* used nine sampling locations with nutrient and algal parameters

measured monthly from 2009-2011 to show the variability of the system. They found that inter-annual differences in nutrient and microcystin concentrations could be explained by NPS pollution mitigating strategies that had been employed, while differences in water quality throughout the lake showed that the effect of mitigating strategies had a spatial element.

Work has been done on assessing spatiotemporal dynamics of pollutants in rivers, too. In an in-depth look at water quality in rivers at different spatial scales, Casper *et al.* (2012) found that rivers are not the homogeneous and well-mixed water bodies they are often mistakenly regarded as; instead they have heterogeneous and patchy-mosaic structures that relate to land-use at the 300 km scale, surface and ground-water interactions at the 1000 m scale, river-estuarine tidal mechanisms at the 100-1000 m scale, and the effects of physical structures like docks and small sand bars at the 10-100 m scale.

2.4.3. Small water body trends

Small water bodies are complex (Hestir et al, 2015), globally abundant (Downing *et al.*, 2006), and can play prominent roles in freshwater nutrient cycling (Song *et al.*, 2013). A few studies have investigated the spatial dynamics of water quality parameters within small freshwater bodies focused more on high temporal resolution studies and individual small bodies as experimental units. For example, in 2007 Bonachela *et al.* performed a study on 40 irrigation ponds in Southeast Spain, investigating their diurnal oxygen patterns, finding that oxygen depended mostly on photosynthetic activity, and could vary significantly between ponds based on macrophyte composition and the extent of cover on the surface.

Assumptions of homogeneity and the cost and labor of monitoring schemas limits research in small bodies of water, and favors research plans that have high ratio of area:sampling points

(Casper *et al.*, 2012). However, there are mounting evidences to suggest these assumptions are unfounded. In 2013, Song *et al.* (2013) found that shallow urban ponds in Ontario, Canada exhibited thermal stratification that correlated with nutrient stratification. Van der Merwe and Price (2015) used infra-red remote sensing to demonstrate that cyanobacterial blooms were spatially heterogeneous in a small (<3 ha) pond. Important new developments in monitoring tools and techniques may help to shed light on the small-scale spatial dynamics of water quality parameters.

2.5. Monitoring tools and methods

The existing tools and methods used in water quality studies define the scale of spatiotemporal characterization that research and monitoring programs can examine. Tools are used for collecting water quality samples **(sampling),** or for measuring water quality parameters **(sensing** and **measuring)**. Improvements in technology over the last few decades have helped researchers expand their studies and better understand water quality dynamics.

2.5.1. Traditional manual methods

Traditional manual water quality sampling and sensing are terms for techniques that are carried out by hand, such as grab sampling or sensor measurements. The former is the use of an open container to collect a water sample at a specified depth for analysis on site or in a laboratory (US EPA, 2003), while the latter is the use of optical, temperature, proximal, fluid velocity, electrochemical, or acoustic sensors to measure a target parameter at a fixed measurement location (Wilde, 2008). Traditional manual sampling is generally considered the simplest method of sampling, and it is widely used to different degrees in governmental, volunteer, and research monitoring designs (Heini *et al.*, 2014; US EPA, 2008).

Despite its prevalence, there are limitations to what manual sampling can accomplish. Manual sampling introduces a human element which can increase error and sampling bias (Costello *et al.*, 2009; Davies and Mazumder, 2003); it can be expensive in terms of equipment, laboratory analysis, and labor-hours (Robertson and Roerish, 1999); and it can be spatially unrepresentative (Hestir *et al.*, 2015). Creating a sampling design using statistical sampling theory (Gruijter *et al.*, 2006) is one way to overcome the lack of representativeness of a small number of sampling points, but it has been shown that sampling strategies can have a substantial impact on the conclusions drawn from data (Cooper, 2004), and can overlook potentially important dynamics in water (Casper *et al.*, 2012).

2.5.2. Remote sensing

With the introduction of remote sensing, larger bodies of water can be quickly assessed at improved spatial resolutions. **Remote sensing** is a method of environmental sampling that is used to collect data on areas or objects based on reflected light and energy captured by different instruments - typically aboard drones, airplanes, and satellites (NOAA, 2015). Instruments can measure target parameters passively – by measuring naturally reflected or emitted radiation - or actively – by emitting radiation and measuring returning reflectance (Graham et al, 1999). With ever-improving capabilities, remote sensing has been used to assess a variety of parameters including a strong focus on chlorophyll and cyanobacteria concentrations (Becker *et al.*, 2009; Gomez *et al.*, 2011; Han and Jordan, 2007; Torbick, 2013), macrophyte concentrations (Matthews *et al.*, 2010), phycocyanin, dissolved organic matter (Becker *et al.*, 2009), total suspended matter and transparency (Budd and Warrington, 2004; Chipman *et al.*, 2004; Ma and Dai, 2007), fecal coliforms (Kotchie *et al.*, 2015), and hydrologic parameters like discharge (Bjerklie *et al.*, 2003; Smith *et al.*, 1996).

However, in a review on current trends in remote sensing, Hestir *et al.* (2015) highlighted some of the major limitations of remote sensing methods including limitations on size (lakes greater than 0.01 km^2 cannot be analyzed by low spatial resolution satellite remote sensing), measured parameters (no direct method to measure nitrogen and phosphorus concentrations), and temporal resolution. The latter limits the use of remote sensing applications for monitoring rapid biological processes like the sudden onset of HABs.

Remote sensing for small or complex freshwater systems can overcome the spatial and temporal limitations of satellite remote sensing by using drones and other unmanned aerial vehicles (UAVs) as platforms for sensing and imaging equipment. According to a review by DeBell *et al.* (2015), the potential of UAVs for environmental sensing has been acknowledged since 1993, but it has only been in the past few years that UAVs have become affordable for widespread monitoring use. Recently, UAVs have been used to map and track oil spills (Fingas and Brown, 2014), sediment pollution (Zang *et al.*, 2012), stream temperatures (Deitchmann, 2009), aquatic vegetation distribution (Flynn and Chapra, 2014; Husson *et al.*, 2013), river hydromorphology (Casado *et al.*, 2015), and small-scale cyanobacterial dynamics (Van der Merwe and Price, 2015). Furthermore, Lega *et al.* (2012) demonstrated how UAVs could be used to assess dynamic polluting sources, by capturing multispectral and infrared images that highlighted illegal sewage discharge from a moving ship. Though UAVs have many applications for water quality monitoring, indirect sensing is not a practical method for measuring concentrations of some key pollutants – particularly constituents of diffuse NPS nutrient pollution.

2.5.3. Automated methods and proximal sensing

Automated sensing and sampling technologies can perform *in-situ* measurements or sample collection at fixed, discrete locations. Automated sensing is an arm of **proximal sensing,** which is any environmental sensing that takes measurements closer than 2 m from the target surface (Rossel *et al.*, 2010). Automated sensing and sampling are an improvement over traditional manual methods because they remove sampler bias, reduce labor hours, and can drastically improve temporal resolution by allowing for real-time continuous sensing and sampling (Glasgow *et al.*, 2004). In a review of the currently implemented technologies, Glasgow *et al.* described how automated sampling tools are used world-wide, including water column profilers in Delaware, USA; deep-water platforms in Bermuda measuring current speed, temperature and conductivity measurements; and flow-through measurement devices attached to merchant ships in the Baltic Sea. Automated sampling can be used effectively for high-quality temporal sampling at discrete sampling points, but due to the high cost of these technologies, it can be even less spatially representative than manual sampling (Robertson and Roerish, 1999).

2.5.4. Unmanned vehicles for proximal sensing

Unmanned surface vehicles (USVs) and automated underwater vehicles (AUVs) are mobile sensor platforms that can perform sample collection and automated measurements of water quality parameters. Their movement can be remotely controlled, or completely automated. Their mobility increases spatial representativeness of monitoring schemas, and can be used to perform high-accuracy transects through water to map the spatial structure of target parameters (Dunbabin and Grinham, 2010). Due to the relatively recent application of unmanned vehicles for freshwater quality monitoring, most work on USVs or AUVs focus on their design, navigation, guidance, and control. Recent developments have focused on autonomous, intelligent

navigation (Huntsberger and Woodward, 2011) and solar-powered systems for long-duration missions (Garcia-Cordova and Guerrero-Gonzalez, 2013).

Several studies have used USVs and AUVs for spatial mapping of water quality parameters. In a 2008 technology demonstration of the YSI ecomapper AUV, Ellison and Slocum demonstrated that a submersible vehicle with a suite of sensors measuring temperature, depth, dissolved oxygen, and chlorophyll fluorescence could effectively conduct transects throughout a 4,900 acre eutrophic lake and produce surface water quality maps. Casper *et al.* (2012) showed that USVs could also produce high spatial resolution maps of surface water quality, and that they were a useful tool in assessing spatial dynamics of DO, chlorophyll fluorescence, conductivity, temperature, turbidity, and dissolved organic matter reflectance.

New technologies based on remotely operated or automated vehicles can improve our capacity for small-scale monitoring in water. However, these vehicles are often designed and tested for large-scale monitoring objectives, and less often for small-scale monitoring. Despite the complexities and ecological importance of small water bodies, assumptions of homogeneity and the cost and labor of monitoring schemas limits the implementation of remote and automated vehicles for high-resolution spatial mapping of water quality constituents. Assumptions of homogeneity must be tested, and work must be completed to develop low-cost solutions for freshwater unmanned surface vehicles that can support small-scale water quality monitoring.

3. Materials and Methods

3.1. Site description

The study was carried out in two connected agricultural drainage ponds, each with a surface area of approximately 0.2 ha. They are located at the Macdonald Campus of McGill University in Sainte-Anne-De-Bellevue, Quebec, and Canada – approximately 40 km west of downtown Montreal, QC (Fig. 3.1).

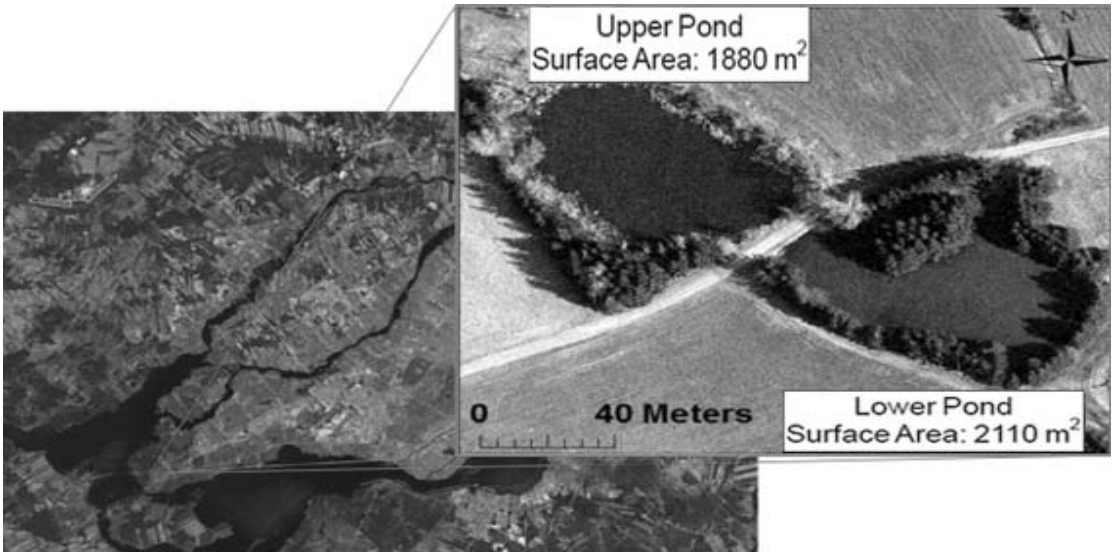

Fig. 3.1. Study ponds in Ste-Anne-De-Bellevue, Quebec.

Cumulatively, these ponds are fed by six sub-surface tile drains and two open-air collector drains, which drain five agricultural fields. These fields comprise a cumulative area of nearly 19 ha, though each plot had its own unique fertilizer application (Table 3.1) and crop management (Fig. 3.2). The surrounding agricultural watershed has highly variable soil and as is typical for the St-Lawrence lowland area, the soils are mostly acidic loam soils (IRDA, 1971). However, the ponds have a clay-rich foundation and 5-10 m vegetation buffer comprising a riparian strip of semi-submerged aquatic vegetation dominated by tall grasses, and terrestrial vegetation dominated by deciduous and evergreen trees.

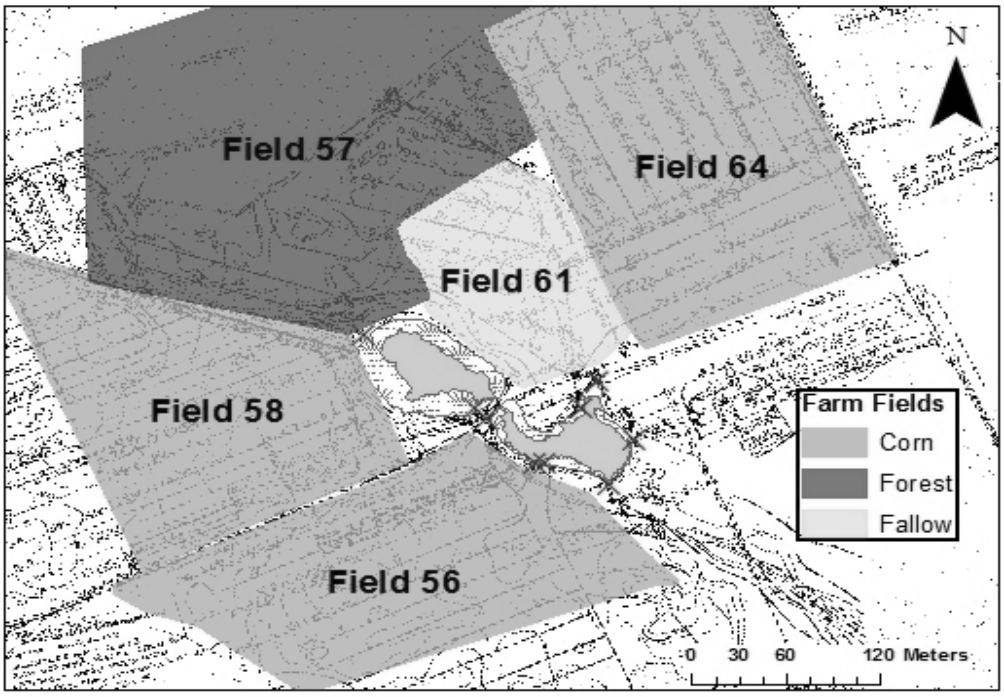

Fig 3.2. Drainage and agricultural management of pond watershed with 2014 fertilizer loads.

Table 3.1. Fertilizer application of surrounding agricultural watershed in 2014. Percent composition of nitrogen (N), phosphorus (P), and potassium (K) is listed in parentheses under the fertilizer applied column (N-P-K).

Field	Date	Fertilizer	Rate kg ha^{-1}	kg N ha^{-1}	kg P ha^{-1}
Field 58	15-May	28-26-0	151	42	39
	19-Jun	27-0-0	425	114	0
		46-0-0	225	103	0
Field 56	23-May	46-0-0	200	92	0
		46-0-0	75	34	0
Field 61	8-May	21-0-0	150	31	0
Field 64	21-May	46-0-0	175	80	0
	23-May	46-0-0	75	34	0

The upper pond (UP) (Fig. 3.1) drains into the lower pond (LP) via a 0.33 m culvert. Oblique images of the pond surfaces were taken on three times a week from a single reference point to illustrate the growth patterns of duckweed (genus *Lemna*) through the summer (Fig. 3.3). The UP surface became completely covered by the beginning of June, while the LP did not experience significant growth of duckweed until the end of July.

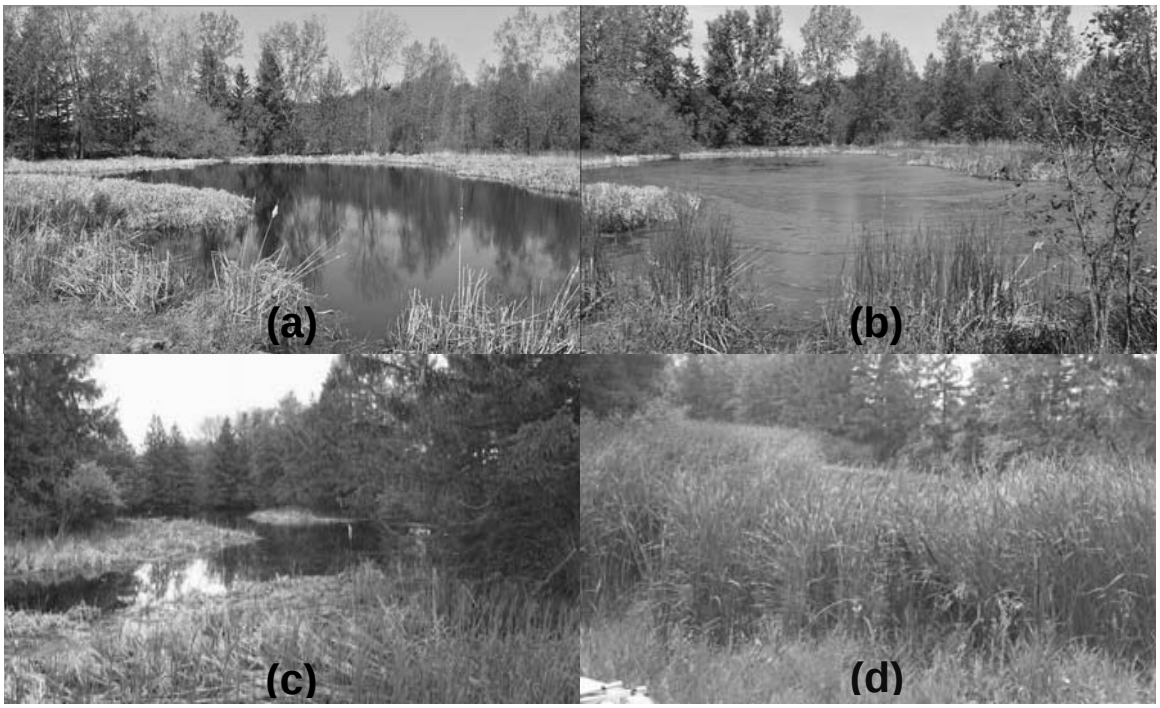

Fig. 3.3. Oblique images of vegetal surface change for both study ponds. (a) UP, May 28; (b) UP, June 01; (c) LP, May 28; (d) LP, August 07.

3.2. Pond bathymetry and discharge

The quantitative measure of the volume in the two ponds was determined by sampling at 45 sampling points in each pond twice between May and August 2015. Water depth was measured using a four-meter sounding line. Precipitation data were collected from the J.S. Marshall Radar Observatory (WMO ID#71377) located 0.5 km east of the site. Discharge from the LP was calculated using the Kindsvater-Carter rectangular weir equation (ISO, 1980):

$$Q = C_e \frac{2}{3}\sqrt{2g}(b + K_b)(h + K_h)^{\frac{3}{2}} \quad (3.1)$$

where

Q = Discharge ($m^3 s^{-1}$)
C_e = Discharge coefficient
g = Acceleration of gravity ($m s^{-2}$)
b = Notch width (m)
K_b = Effect of viscosity tension (m)
h = Head (m)
K_h = Effect of surface tension (m)

The sum b + K_b is the "effective width" and the sum h+K_h is the "effective head". C_e is a function of b/B and h/P, and K_b is a function of b/B (where B = channel width). Discharge can be calculated using the International Standards Organization's 1980 graphs for effective width and head (ISO, 1980). The composition of inflow water from surface runoff and subsurface drainage was estimated using the Web-based Hydrographic Analysis Tool (WHAT) (Lim *et al.*, 2005)**.** An ephemeral model was selected to most closely model pond hydrology (Fig. 3.4).

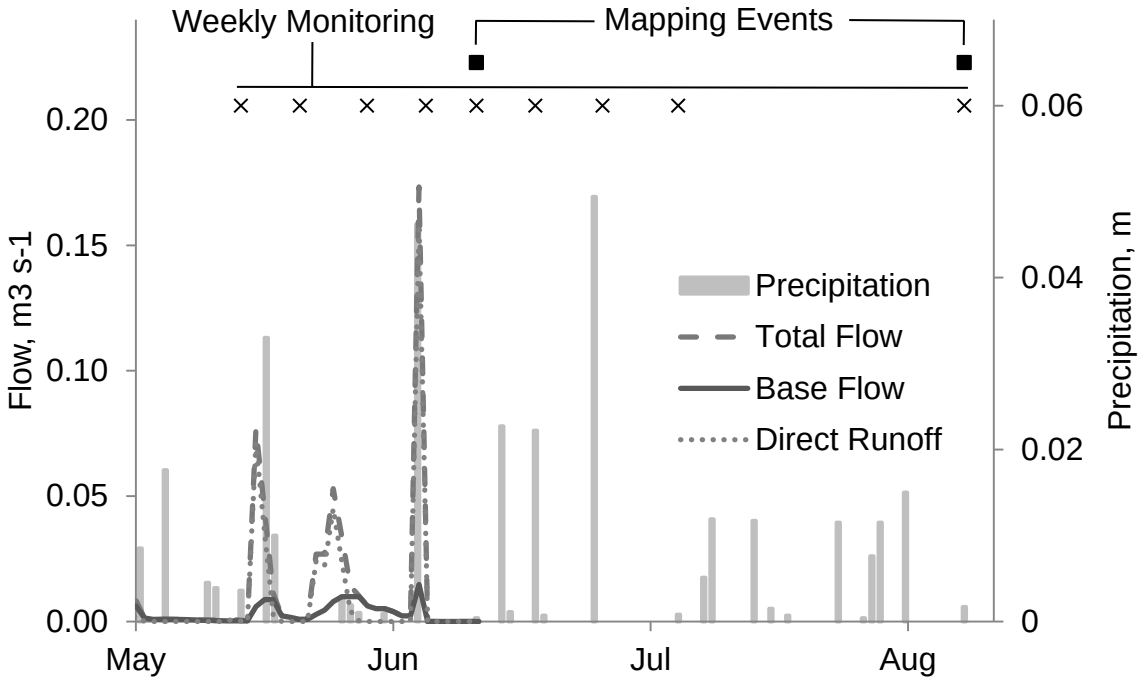

Fig 3.4. Precipitation (measured), direct runoff from surface and subsurface drains (estimated), and groundwater base flow (estimated) during the 2014 sampling season.

3.3. Sampling design

The monitoring protocol was designed to obtain a characterization of the spatiotemporal dynamics of environmental water quality indicators by quantitative measure of the temperature (ºC), pH, total concentration of Dissolved Oxygen (DO) (mg L^{-1}), and the concentrations of Total Nitrogen (TN) (mg L^{-1}), Particulate Nitrogen (PN) (mg L^{-1}), Total Dissolved Nitrogen (TDN) (mg L^{-1}), Total Ammonical Nitrogen (TAN) (mg L^{-1}), Nitrate-Nitrogen (NO_3^--N) (mg L^{-1}),

Dissolved Organic Nitrogen (DON) (mg L^{-1}), Total Phosphorus (TP) (mg L^{-1}), Total Dissolved Phosphorus (TDP) (mg L^{-1}), Dissolved Reactive Phosphorus (DRP) as Ortho-Phosphate (Ortho-P) (mg L^{-1}), Dissolved Organic Phosphorus (DOP) (mg L^{-1}), and Particulate Phosphorus (PP) (mg L^{-1}). Weekly monitoring of twelve control locations was pursued for eight weeks from May 08 to July 04, 2014 (Fig. 3.5); control locations were selected following a stratified random sampling design in which stratification relied on the ancillary information derived from the agricultural watershed management and drainage locations (Fig. 3.2).

Weekly monitoring was complemented with two dense water sensing events – one in June and one in August - following a grid sampling design to capture spatial distributions of T, DO, pH, and NO_3^--N. Each mapping event was completed in two days except for the June mapping event in the LP, which took four days. Due to a sensor malfunction, DO was only mapped for the August sampling event in both the UP and LP. Apart from physical barriers to sampling like emergent aquatic vegetation, the major inherent challenge to spatial snapshots of water quality is that sampling must occur during a small enough time range such that parameters are negligibly changing throughout the sampling period.

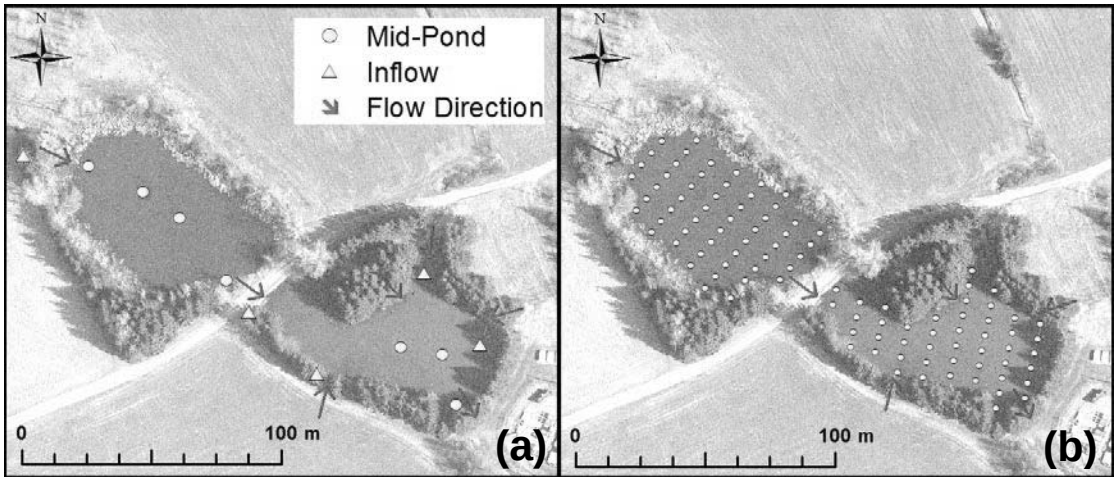

Fig. 3.5. Sampling points for locations of 12 control points (a) and sampling points for dense sampling events (b). The UP outlet is connected to one of the LP inflows via a 0.33 m culvert beneath the road.

3.4. Data collection

For all measurements and sample collection, a 1.8 m long inflatable raft was used to reach control locations in the ponds, where necessary. Each of the twelve control locations were marked with a make-shift buoy of recycled materials.

3.4.1. Proximal sensing

A suite of sensors was used to measure the total concentrations of water quality constituents (Table 3.2). For weekly and complementary dense sampling events, DO and T were measured using a Galvanic DO electrode (9551-20D, Horiba Ltd., Tokyo, Japan), pH was measured using a glass pH electrode (PY-P21, Denver Instrument/Sartorius, Inc., Bohemia, NY, USA), and NO_3^--N was measured using a combination, PVC membrane nitrate electrode (Nico Sensors, Inc., Huntingdon Valley, PA, USA). Nitrate-nitrogen measurements were validated *ex-situ* using a spectrophotometric method on a Lachat Quikchem® 8500 Flow Injection Analysis System (Table 3.2). Prior to each sampling session, each sensor was calibrated according to manufacturer recommendations. The DO sensor was calibrated using a two-point calibration containing Sodium Sulfite (Na_2SO_3), the pH sensor was calibrated using a three-point calibration and standard buffers, and the nitrate sensor was calibrated using a six-point calibration of NO_3^- as sodium nitrate ($NaNO_3^-$) solution. One measurement was taken at each sampling location. After each measurement, each sensor was rinsed with distilled, double-deionized water (Milli-Q system®, Millipore, Molsheim, France).

Table 3.2. Summary of parameters and analytical techniques used during data collection.

Analytical Technique	Sampling Event	Observations	Parameters	Units
Electrochemical	Weekly; Grid Weekly; Grid	*in-situ*	pH, DO, NO_3^--N	pH unit, mg L^{-1}
Thermal resistance	Weekly; Grid	*in-situ*	T	^oC
Spectrophotometric	Weekly	*ex-situ*	TN, TDN, NO_3^--N, TAN, TP, TDP, DRP	mg N L^{-1}, mg P L^{-1}
Calculated	Weekly	*ex-situ*	DON, PN, DOP, PP	mg N L^{-1}, mg P L^{-1}

3.4.2. Laboratory analyses

Samples were collected and analyzed in the laboratory to measure the total concentrations of TN, PN, TDN, NO_3^--N, TAN, DON, TP, TDP, PP, DOP, and DRP for the weekly sampling events. Three randomly selected 125 mL samples were collected at 0.1 m below the pond surface within a one meter radius of each buoy by grab sampling, and the samples were stored in 125 mL white plastic HDPE bottles (Nalgene®, Thermo Fisher Scientific Inc., Waltham, MA, USA) in a cooler packed with ice. All containers used for this study were rigorously pre-washed using the following protocol: three cycles of hot water, one cycle of phosphate-free detergent (*Sparkleen*®, Thermo Fisher Scientific Inc., Waltham, MA, USA) solution, three cycles of hot water, three cycles of distilled water, an overnight soaking in an HCl acid-bath solution (~10%), a single rinse with distilled water, and a final rinse with distilled, deionized Millipore water.

Upon return from the field site, all samples were immediately filtered using a 0.45 micron nylon filter (Thermo Fisher Scientific, Inc., Waltham, MA, USA). Cellulose filters were not used as they were determined to add trace amounts of nitrogen to samples, during preliminary lab experiments. All analyses were completed on the Lachat analyzer. Detection limits varied from

0.01-0.3 mg P L^{-1} or mg N L^{-1}. Aliquots of 5 mL in volume of filtered and unfiltered sample were digested following the persulfate digestion method of Ebina *et al.* (1983) to determine the concentration of TN, TDN, TAN, NO_3^--N, TP, TDP, and DRP (Fig. 3.6). Concentrations of the particulate forms of N and P were calculated as the difference between the total concentrations and total dissolved concentrations, and the organic forms were calculated as the difference between the total dissolved concentrations and the measured inorganic concentrations (Kovacic *et al.*, 2000).

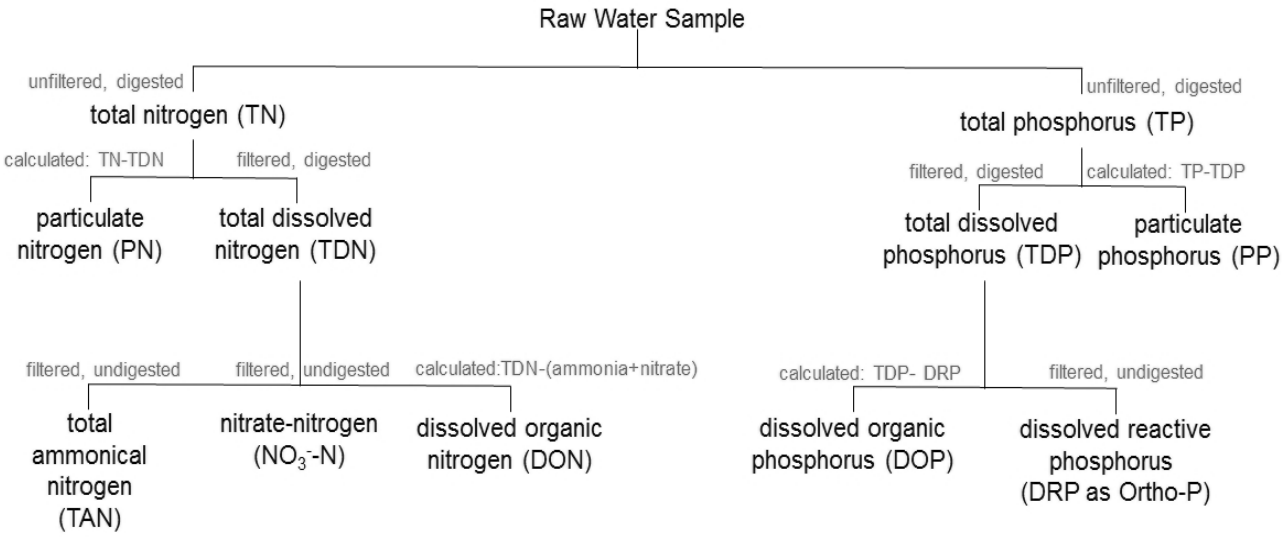

Fig. 3.6. Filtration and digestion schemes for the measured forms of nitrogen and phosphorus.

3.5. Data analyses

3.5.1. Temporal Analysis

Data outliers and erroneous measurements (from sensor errors or calibration errors) were removed. Raw mV values recorded by the nitrate sensor were converted to mg N L^{-1} by preparing a log-scale calibration curve (US EPA, 2012b). Calibration curves were calculated each sampling day using fresh standards, and the corresponding slope and intercepts determined from the calibration curve. For the temporal trend analyses of nutrients, Inverse-Distance

Weighting (IDW) was applied to smooth the data and create a predicted trend-line. IDW was calculated based on Shepard's basic method for one dimension.

3.5.2. Statistical comparisons

A statistical model with nested fixed effects using least-square means (LS means) was used on a subset to determine the effect of pond, temporal, and proximity to inflows on each water quality constituent (Equation 3.2). The data were subset into groups to improve the balance of the analysis; the subsets comprised three weeks before the rapid onset of duckweed, and three weeks after. Each of the three effects was considered as a binary factor with two possible levels: Pond ("UP" for upper pond or "LP" for lower pond); Time (either "Before" for before the duckweed growth event or "After" for after the duckweed growth event); Location (either "inflow" for measurements at pond inflows, or "pond" for measurements within the body of the pond but away from the inflows, also referred to as "mid-pond").

Since each experimental unit had a combination of all possible levels of the three factors, and the effects were not all independent from each other (location is nested within pond), the experiment was considered to have a factorial design and the effects of factors were assessed by looking at the three-way interaction between the factors (Dutilleul, 2011). There were three factors each with two levels (2^3), so eight different experimental units were assessed (i.e., before*UP*inflow, before*LP*inflow, after*UP*mid-pond, etc.).

R statistical software (R Foundation for Statistical Computing, Vienna, Austria) was used to assess the model. LS means were used to conduct significant groupings based on Tukey-adjusted pairwise Student's t-test. Based on the pair-wise comparisons, significance groupings were

determined for each parameter. Treatments that are not significantly different from each other are denoted with the same alphabetical letter.

$$Y_{ijk} = \mu + \text{time}_i + \text{location}_{jk} + \text{time} * \text{location}_{ijk} + \varepsilon_{ijk} \quad (3.2)$$

where

Y_{ijk} is the measured concentration or activity of the target water quality parameter at the k^{th} location in the j^{th} pond during the i^{th} time level

time_i is the fixed effect of the i^{th} time period (before $i = 0$, and after $i = 1$)

pond_j is the fixed effect of the j^{th} pond (upper pond $j = 0$, and lower pond $j = 1$)

location_{jk} is the fixed effect of the k^{th} location (inflow $k = 0$, and mid-pond $k = 1$) nested in the j^{th} pond

3.5.3. Spatial Analysis

For the spatial analyses of the grid sensing events, ordinary kriging (Oliver, 1990) was performed using the ArcGIS version 10.0 (ESRI, San Diego, CA, USA) to create an interpolated 2-D raster layer from point data. Data distributions were checked for normalcy using the histogram and QQ-plot tools in the ArcGIS Geostatistical Wizard. Nugget and sill parameters were reported for the semivariogram models produced for each measured parameter in each sampling event. Parameters with a Nugget/sill ratio below 0.25 are considered to have strong spatial dependence; between 0.25 to 0.75 are considered to have moderate spatial dependence; and greater than 0.75 are considered to have weak spatial dependence (Sun *et al.*, 2003).

Spatial and temporal analyses are applied in this study to investigate if an approach combining dense spatial mapping and weekly temporal monitoring at a select number of points will improve small-scale monitoring of freshwater bodies. Dense spatial sampling is proposed as a means to

determine the spatial dynamics of target water quality parameters and to indicate polluting hotspots or areas of spatial heterogeneity. Spatial analyses would then be used to determine if it is beneficial to select sampling locations for continuous temporal monitoring based on the water quality maps produced from dense spatial mapping. Weekly temporal monitoring can then be used to capture temporal dynamics in the system without concern of missing spatial dynamics.

4. Results & Discussion

4.1. Time analysis

4.1.1. Duckweed, T, DO, and pH

Duckweed was sparse in the both ponds and covered less than 5% of the pond until 28 May - then it rapidly grew in the UP (Fig 3.3). By 01 June, duckweed covered 100% of the surface area of the UP and formed a mat for the remainder of the season that became thicker through the summer (Fig. 3.3). This rapid surface growth only occurred in the UP, and is referred to as the Duckweed Growth Event (DGE). In the LP, pond cover remained at 5% - 10% through and up to 04 July, increasing to 60% - 70% surface coverage by 10 August (Fig. 3.3). In part, this difference in surface vegetation can be attributed to both the shallow nature of the UP - which had a maximum depth of 1.7 m (measured on 25 June) compared to the LP with a maximum depth of 3.5 m (measured on 25 June) – and the decreased canopy coverage in the UP (Fig. 3.1).

Water temperature increased throughout the summer in both ponds, from 16.3 ± 0.23^{o}C to 19.6 ± 0.31^{o}C in the UP, and 14.9 ± 0.27^{o}C to 22.7 ± 1.7 ^{o}C for the LP from the first week of May to the first week of August (Fig. 4.1). The two ponds had similar temperatures until August, when the LP temperatures were higher. The LS means analysis confirmed that although temperatures were higher after the DGE, there was no temperature difference between the two ponds immediately before and after the DGE (Table 4.1).

Water temperature can be affected by duckweed growth, as thick duckweed mats have increased albedo by reflecting sunlight and reduce the amount of solar radiation that can reach the water column (Dale and Gillespie, 1976). In May and June, the duckweed mat in the UP was unlikely to be thick enough to have a significant albedo, and there was constant flowing water from snowmelt and drainage inflows that further reduced the effect of the duckweed mat on

temperature (Rutherford, 1997). By August, the duckweed mat was much thicker in the UP and flow had ceased by 04 July (discounting occasional flow linked to precipitation events) (Fig. 3.4), leading to lower temperatures in the UP as compared to the largely uncovered LP.

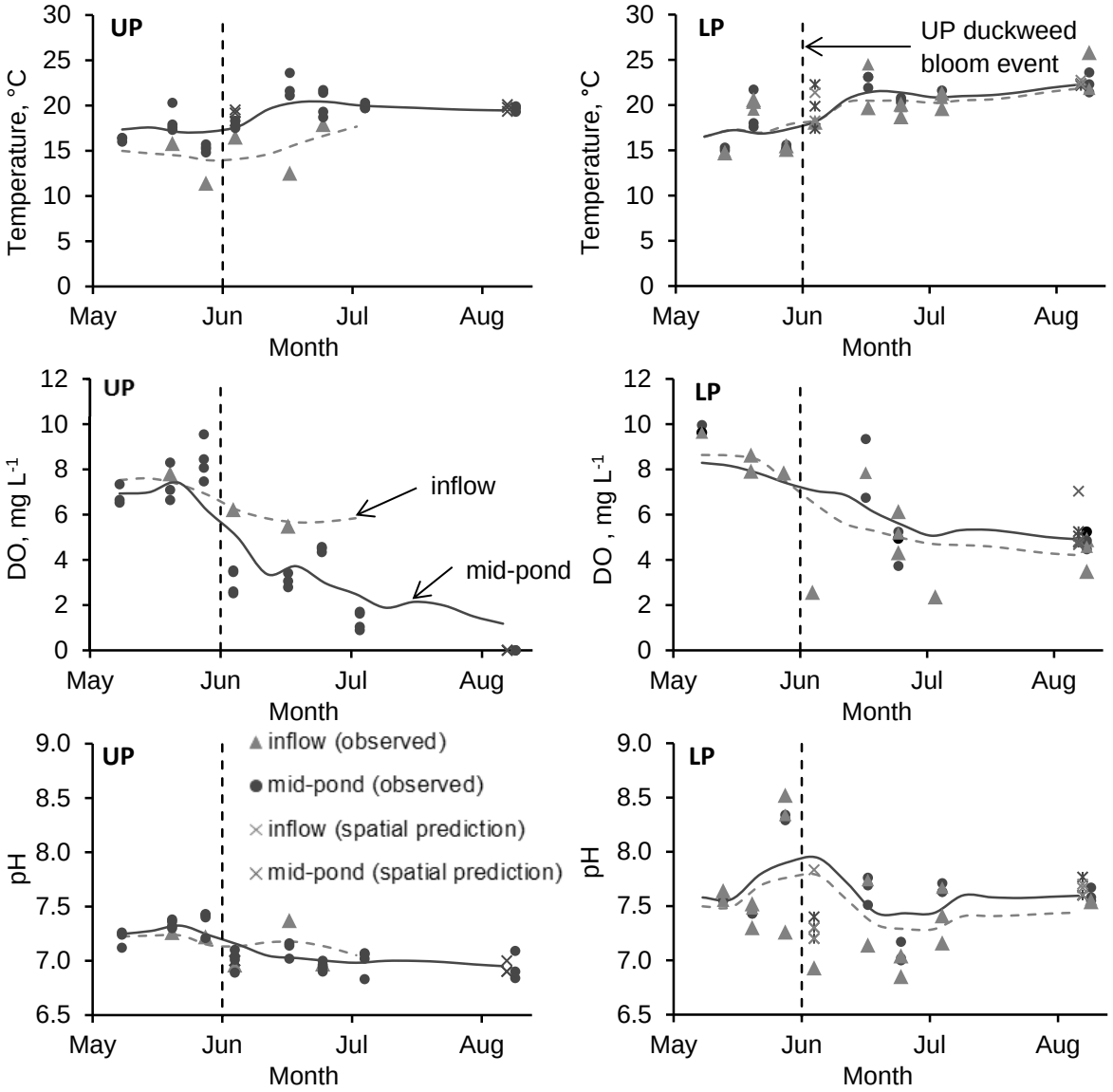

Fig. 4.1. Time trends in water quality constituents, pH, T, and DO, for May-August. IDW trend-line predictions are shown as lines.

Dissolved oxygen (DO) decreased in both ponds, from 6.84 ± 0.44 to 0.0 ± 0.0 mg L^{-1} in the UP and 9.63 ± 0.27 to 5.26 ± 0.89 mg L^{-1} in the LP (Fig. 4.1). In the UP, DO initially increased until

the DGE, which was driven by increased photosynthesis from the rapidly growing duckweed (Zimmo, 2003). Immediately after the DGE, DO sharply decreased mid-pond and continued to steadily decline to 0.0 mg L^{-1} by 08 August. The LS means analysis confirmed that there was a significant decrease in DO immediately after the DGE (Table 4.1). Grouping A comprised the three lowest LS means, which all occurred after the DGE (LP*inflow*after, UP*inflow*after, and UP*pond*after) indicating that concentrations were significantly lower after the DGE. In the LP, the LS means analysis also indicates that there was a significant decrease in DO after the DGE – as grouping B is significantly different from grouping D.

Decreases in DO concentrations occur primarily when oxygen depletion from respiration occurs faster than reoxygenation from photosynthesis and air-surface gas exchange. In eutrophic freshwater systems, nutrient enrichment drives rapid phytoplankton bloom and decay, leading to oxygen-consuming decomposition (Rabalais *et al.*, 2010). However, duckweed generations are roughly 18 days at their shortest (Hillman, 1961), so it is unlikely that their decay was a significant driver of the sharp decrease in DO immediately after the DGE; more likely, a combination of increasing temperatures causing the solubility of oxygen to decrease (Weiss, 1970), and reduced surface gas exchange due to the physical cover of duckweed drove DO depletion (Bonachela *et al.*, 2007). Additionally, the physiology of duckweed may have played a role in the decline of DO - oxygen consumption during respiration occurs at the submerged roots of the duckweed, while oxygen produced during photosynthesis is released into the atmosphere from the stomata, located on the unsubmerged leaf surface of the duckweed (Hillman, 1961).

Table 4.1. Significance groupings and LS means analysis of T and DO. LS means are ordered from high to low.

Parameter	Time	Pond	Location	LS means	SE*	Groupings			
T (°C)	After	LP	mid-pond	21.6	0.8		B		
	After	UP	mid-pond	21.1	0.8		B		
	After	LP	inflow	20.7	0.8		B		
	Before	LP	mid-pond	16.7	0.7	A			
	Before	LP	inflow	16.6	0.6	A			
	Before	UP	mid-pond	16.6	0.6	A			
	After	UP	inflow	15.2	1.4	A			
	Before	UP	inflow	13.6	1.4	A			
DO (mg L^{-1})	Before	LP	mid-pond	9.8	0.9				D
	Before	LP	inflow	8.7	0.6				D
	Before	UP	inflow	7.8	1.3		B	C	D
	Before	UP	mid-pond	7.6	0.4			C	D
	After	LP	mid-pond	6.0	0.6		B	C	
	After	UP	inflow	5.5	1.3	A	B	C	D
	After	LP	inflow	5.4	0.6	A	B		
	After	UP	mid-pond	3.7	0.5	A			

* standard error

pH trends were markedly different in the UP and LP, which was confirmed by the prominent pond effect in the LS means analysis (Table 4.2). In the UP, there was a gradual decrease in pH until the 3rd week of June - from 7.21 ± 0.08 to 6.94 ± 0.13 – after which it was almost constant until 10 August (Fig. 4.1). In the LP, the pH was consistently higher than the UP. At the beginning of the season it was an average 7.56 ± 0.05 and sharply rose to 8.36 ± 0.08 on the 28th of May, immediately prior to the DGE in the UP. The pH in the LP reached a low of 7.07 ± 0.08 on the 25th of June, then rose to 7.58 ± 0.04, nearly the same pH as at the beginning of the May. pH is closely related to photosynthetic activity in aquatic systems (Staehr *et al.*, 2012). The duckweed mats inhibit photosynthetic activity of phytoplankton in the water column, causing pH to remain relatively low and constant during the season (Zimmo, 2003).

Table 4.2. Significance groupings and LS means analysis of pH. LS means are ordered from high to low.

Parameter	Time	Pond	Location	LS means	SE*	Groupings		
pH	Before	LP	mid-pond	7.8	0.1			C
	Before	LP	inflow	7.7	0.1		B	C
	After	LP	mid-pond	7.4	0.1	A	B	C
	Before	UP	mid-pond	7.3	0.1	A	B	
	After	LP	inflow	7.2	0.1	A	B	
	Before	UP	inflow	7.2	0.2	A	B	C
	After	UP	inflow	7.2	0.2	A	B	C
	After	UP	mid-pond	7.0	0.1	A		

* standard error

4.1.2. Nitrogen

All forms of N were measured from 08 May – 04 July, except for NO_3^--N, which was additionally measured during the August dense sampling event. Nearly all of the nitrogen in the pond waters was dissolved rather than particulate; therefore, TN and PN were omitted from this study.

TDN increased in both ponds but eventually decreased in the UP between 08 May and 04 July (Fig. 4.2). In the UP, TDN was higher at inflow sites than in the pond: inflow TDN increased from 4.08 ± 0.14 to 7.86 ± 0.37 mg N L^{-1}, while mid-pond TDN increased from 2.98 ± 0.19 to 5.49 ± 1.01 mg N L^{-1} on 25 June, but subsequently fell to 1.91 ± 0.41 mg N L^{-1} by 04 July. Higher concentrations in the UP inflow were confirmed by the LS means analysis which determined that UP*inflow*after concentrations of TDN were significantly higher than at other locations (Table 4.3). Higher concentrations of TDN are to be expected at the inflow locations, as the field that drains into the UP – Field 58 (Fig. 3.2) - received N fertilizer in both May and June of 2014 (259 kg N ha^{-1}) (Table 3.1). In Quebec and Ontario, subsurface runoff through tile drainage systems readily carries with it dissolved forms of N (De Jong *et al.*, 2009).

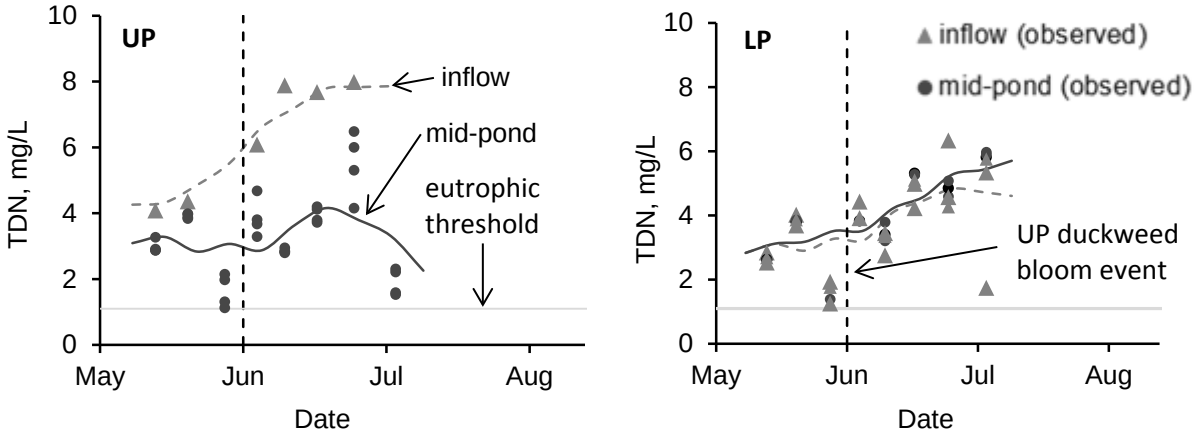

Fig. 4.2. Time trends for TDN from May-June. IDW trend-line predictions are shown as lines.

Table 4.3. Significance groupings and LS means analysis of TDN. LS means are ordered from high to low.

Parameter	Time	Pond	Location	LS means (mg N L^{-1})	SE* (mg N L^{-1})	Groupings			
TDN	After	UP	inflow	7.8	0.6				D
	After	LP	mid-pond	4.5	0.3			C	
	After	LP	inflow	4.4	0.3		B	C	
	Before	UP	inflow	4.2	0.7	A	B	C	
	After	UP	mid-pond	4.1	0.3		B	C	
	Before	LP	mid-pond	3.0	0.4	A	B		
	Before	UP	mid-pond	2.8	0.3	A			
	Before	LP	inflow	2.8	0.3	A			

* standard error

The same trend in high inflow TDN was not observed in the LP (Fig. 4.2). Though the fields that drained into the LP – Field 56, 61, and 64 - were treated with the same amount of N fertilizer as Field 58 (260 kg N ha^{-1}), the timing of fertilizer application was earlier in the LP, which has serious implications for the amount of nutrient transport in runoff (Carpenter *et al*, 1998). Smith *et al.* (2007) showed that the nutrient runoff after fertilizer application reduces rapidly as more days pass between application and precipitation events. There were no precipitation events immediately after fertilizer application on Fields 56, 61, and 64 limiting N loading and runoff

into the LP (Fig. 3.4). In comparison, there was a significant precipitation event four days after the 19 June fertilizer application on Field 58, which caused increased N loading into the UP.

Concentrations of TDN in the LP at both the inflow and mid-pond steadily increased from May to July: from 2.63 ± 0.17 to 4.63 ± 1.94 mg N L^{-1} at inflow and from 2.61 ± 0.01 to 5.89 ± 0.08 mg N L^{-1} at mid-pond locations. Despite reduced N loading from fertilizer application, there was also less assimilation of dissolved N from macrophytes relative to the UP, as indicated by the lack of duckweed and other macrophytes in the LP.

Dissolved nitrogen was mostly NO3^{-}- N (Fig. 4.2 and Fig. 4.3). NO_3^--N concentrations followed TDN trends closely and were higher than the Quebec eutrophic threshold limits for TN 1.1 mg N L^{-1} (Chambers *et al.*, 2012) between 08 May and 04 July (Fig. 4.3). In both ponds, NO_3^--N concentration rose at the beginning of June, but by August both concentrations fell below the eutrophic threshold limit (Fig. 4.3). In the UP, inflow concentrations were consistently significantly higher than mid-pond as confirmed by the LS means analysis (Table 4.4), peaking immediately after the DGE at 6.49 mg N L^{-1} and then falling to 3.11 mg N L^{-1} by 04 July due to N-loading from fertilizer application in late June (Table 3.1). The UP mid-pond measurements increased to 4.54 ± 1.11 mg N L^{-1} immediately after the duckweed event, falling steeply to 0.60 mg N L^{-1} by 04 July. In the LP, NO_3^--N was consistently lower than the UP but did not experience as sharp a decline in concentration after the DGE, so that by 17 June concentrations in the LP were higher than in the UP. LP inflow and mid-pond NO_3^--N did not greatly differ.

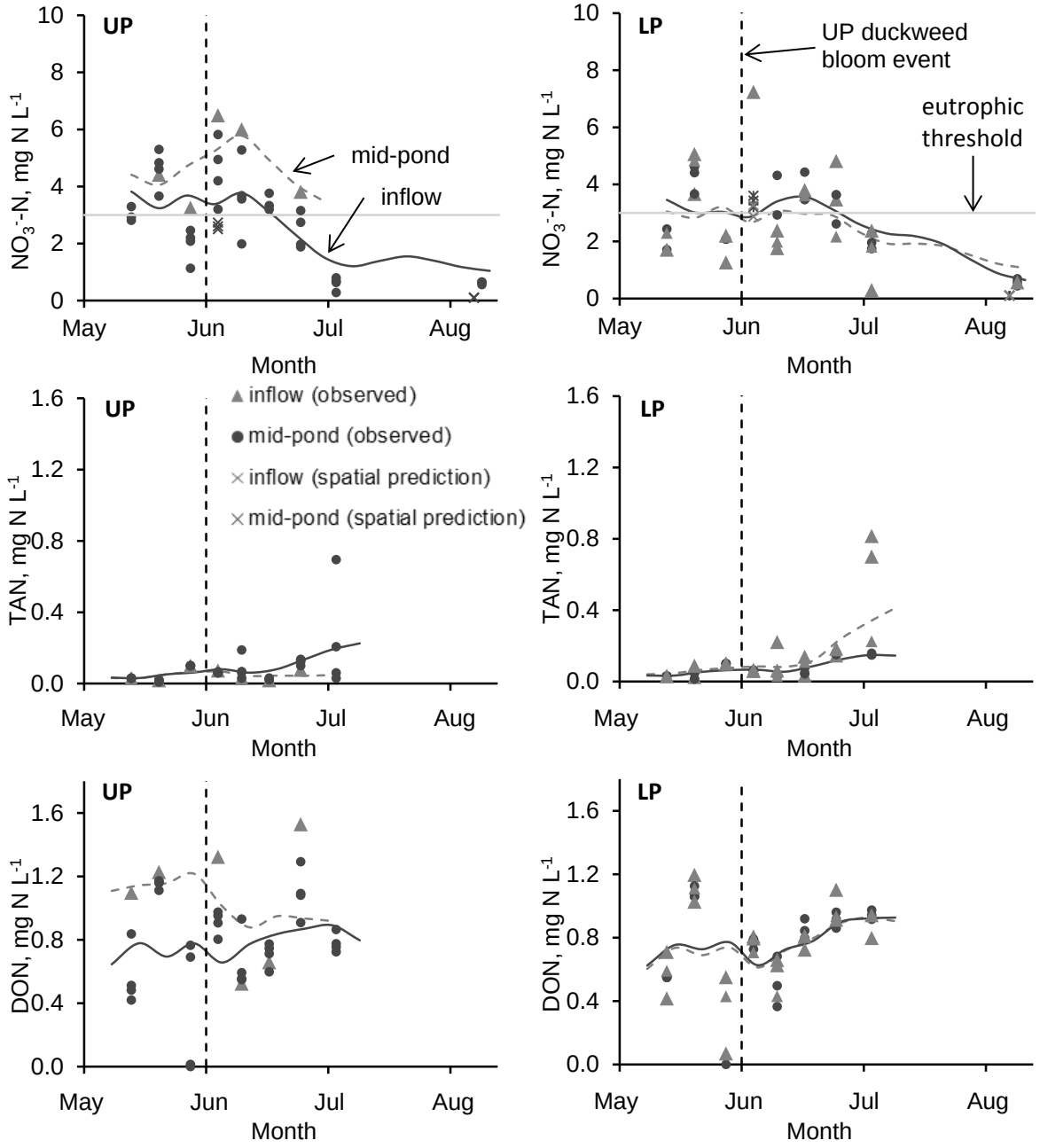

Fig. 4.3. Time trends for the dissolved constituents of nitrogen, NO_3^--N from 08 May - 10 August, and TAN and DON, from 08 May - 04 July. IDW trend-line predictions are shown as lines. It may be noted that NO_3^--N is on a different scale than TAN and DON.

A decrease in NO_3^--N throughout the summer is in line with the findings of Weyhenmeyer *et al.* (2007) and Heini *et al.* (2014) studies on a freshwater lake NO_3^--N concentrations across the summer season. They reported that the reduction in activity is the result of three mechanisms: duckweed and other aquatic macrophytes uptake the bio-available NO_3^--N; the open-air drainage

ditches loading agricultural wastewater into the two ponds dried up by 04 July, leading to reduced N loading; reductions in DO inhibit nitrification, causing less TAN to be oxidized to NO_3^--N. The first mechanism – macrophyte uptake – is the driver of the sharp depletion of NO_3^--N in the UP following the DGE. In a study on N fraction retention in duckweed wastewater ponds, Zimmo *et al.* (2003) found that established duckweed reduced NO_3^--N in a pond by 30%. Other studies have found that duckweed also depletes DO concentrations, causing reduced nitrification (Sartoris *et al.*, 1999).

Table 4.4. Significance groupings and LS means analysis of the NO_3^--N and TAN. LS means are ordered from high to low.

Parameter	Time	Pond	Location	LS means (mg N L^{-1})	SE* (mg N L^{-1})	Groupings		
NO_3^--N	After	UP	inflow	6.90	0.40			C
	After	LP	mid-pond	3.70	0.30		B	
	After	LP	inflow	3.50	0.20		B	
	Before	UP	inflow	3.20	0.40	A	B	
	After	UP	mid-pond	3.20	0.20		B	
	Before	UP	mid-pond	2.10	0.20	A		
	Before	LP	inflow	2.00	0.20	A		
	Before	LP	mid-pond	2.00	0.30	A		
TAN	After	LP	inflow	0.11	0.01			C
	After	LP	mid-pond	0.08	0.01		B	C
	After	UP	mid-pond	0.08	0.01		B	C
	Before	LP	inflow	0.04	0.01	A	B	
	After	UP	inflow	0.04	0.03	A	B	C
	Before	LP	mid-pond	0.04	0.01	A	B	
	Before	UP	mid-pond	0.02	0.01	A		
	Before	UP	inflow	0.02	0.03	A	B	

* standard error

TAN comprised a smaller fraction of TDN than NO_3^--N, and was low throughout the summer with an increase during the last sampling event on 04 July. In the UP inflow, concentrations remained consistently below 0.10 mg N L^{-1}, while mid-pond they rose to an average of 0.25 ± 0.31 mg N L^{-1}. In the LP, TAN concentrations were below 0.15 mg N L^{-1} at inflows and mid-

pond until 04 July, when inflow concentrations rose to an average of 0.46 ± 0.35 mg N L^{-1}. The LS means analysis indicated that TAN significantly increased in both ponds; Grouping A comprises all measurements taken before DGE (in both ponds) as well as the UP inflow measurements after the duckweed (due to high standard error of ±0.03), which are significantly lower concentrations of TAN than Grouping C which comprises all measurements taken after the DGE. The increase in TAN mid-ponds for both UP and LP at the end of the sampling period supports the notion that less nitrification is occurring. In the LP where duckweed slowly grew throughout the summer and DO concentrations did not drop as sharply as in the UP, it is expected that NO_3^--N depletion would also occur less abruptly.

DON ranged from 0.4 to 1.2 mg N L^{-1} in both ponds (Fig. 4.3). In the UP, DON was initially higher at the inflow than mid-pond, but concentrations converged as DON decreased in the UP and increased mid-pond. In the LP, concentrations were not different between the inflows and mid-pond, and had a fluctuating but slight increasing trend from 0.5 to 0.9 mg N L^{-1}. LS means analysis indicated no significant differences between treatments (Table 4.5)

Table 4.5. Significance groupings and LS means analysis of DON. LS means are ordered from high to low.

Parameter	Time	Pond	Location	LS means (mg N L^{-1})	SE* (mg N L^{-1})	Groupings
DON	Before	UP	inflow	1.20	0.20	A
	After	UP	inflow	0.90	0.20	A
	Before	LP	mid-pond	0.80	0.10	A
	After	UP	mid-pond	0.80	0.10	A
	After	LP	inflow	0.80	0.10	A
	After	LP	mid-pond	0.80	0.10	A
	Before	UP	mid-pond	0.80	0.10	A
	Before	LP	inflow	0.70	0.10	A

* standard error

4.1.3. Phosphorus

The ponds had high TN:TP ratios, indicating that the systems are P-limited (Hecky and Kilham, 1988). PP was the largest P fraction in both ponds throughout the study period (Fig. 4.4). In the UP, inflow concentrations of PP decreased from 0.196 to 0.014 mg P L^{-1}, and increased at mid-pond sites from 0.03 ± 0.019 to 0.19 ± 0.10 mg P L^{-1}. In the LP, inflow concentrations rose from 0.02 ± 0.015 to 0.35 ± 0.47 mg P L^{-1} while mid-pond concentrations remained consistently approximately 0.03 mg P L^{-1}.

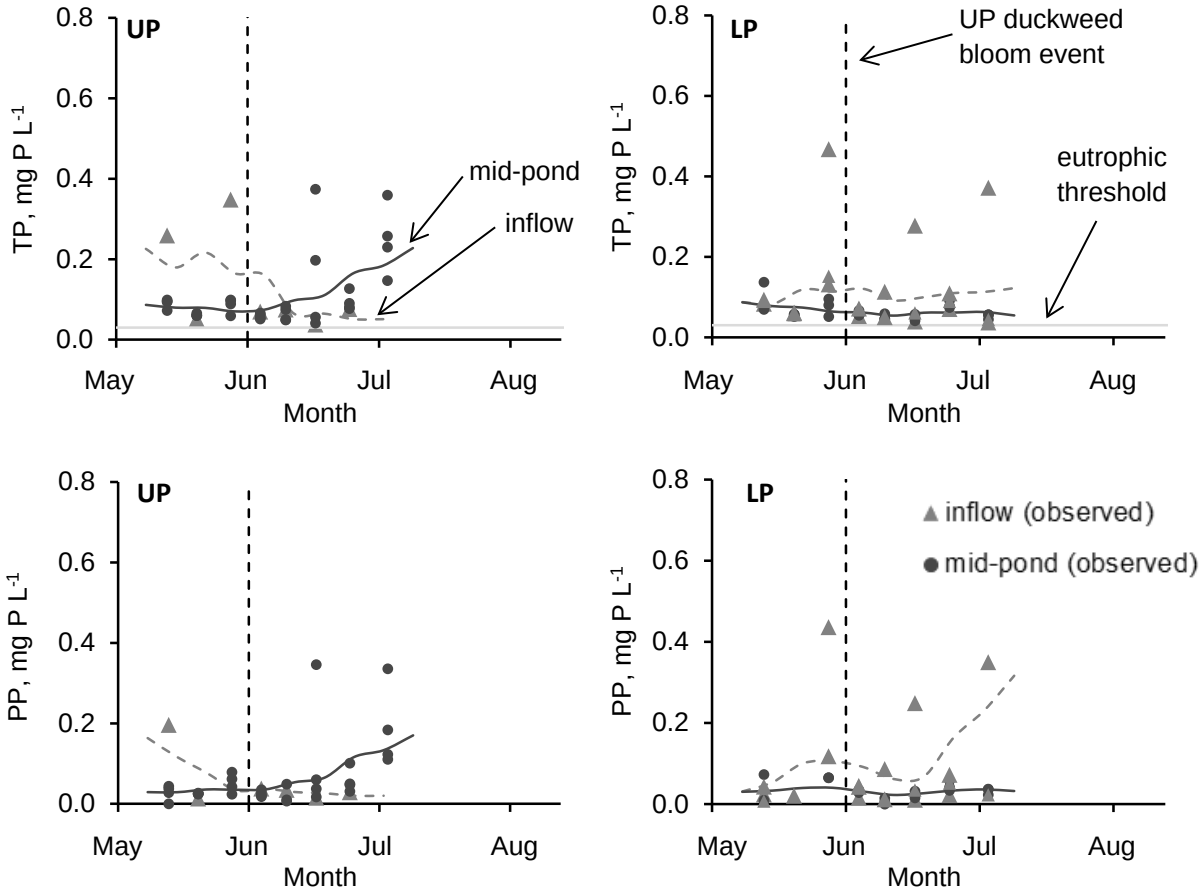

Fig 4.4. Time trends for TP, TDP, and PP from 08 May - 04 July. IDW trend-line predictions are shown as lines. It may be noted that TDP is on a different concentration scale than PP and TP.

Phosphorus is less soluble than N, causing P load to often be particulate in nature (Arheimer and Lidén, 2000). The LS means analysis did not find any significant differences in PP

concentrations due to the DGE, pond, or proximity to inflow likely due to a higher standard error for each treatment (Table 4.6).

Table 4.6. Significance groupings and LS means analysis of TP and PP. LS means are ordered from high to low.

Parameter	Time	Pond	Location	LS means (mg P L^{-1})	SE* (mg P L^{-1})	Groupings	
TP	Before	UP	inflow	0.22	0.04		B
	Before	LP	inflow	0.12	0.02	A	B
	After	UP	mid-pond	0.11	0.02	A	B
	After	LP	inflow	0.10	0.02	A	B
	Before	UP	mid-pond	0.08	0.02	A	B
	Before	LP	mid-pond	0.07	0.02	A	B
	After	UP	inflow	0.06	0.04	A	B
	After	LP	mid-pond	0.06	0.02	A	
PP	Before	UP	inflow	0.11	0.05	A	
	Before	LP	inflow	0.08	0.02	A	
	After	UP	mid-pond	0.06	0.02	A	
	After	LP	inflow	0.06	0.02	A	
	Before	UP	mid-pond	0.03	0.02	A	
	Before	LP	mid-pond	0.03	0.03	A	
	After	UP	inflow	0.03	0.04	A	
	After	LP	mid-pond	0.02	0.02	A	

* standard error.

Both ponds also had similar trends for TDP for most of the summer (Fig. 4.5), confirmed by the LS means analysis that indicates there were no significant differences between treatments for TDP (Table 4.7). In the UP, inflow concentration of TDP decreased from 0.06 to 0.02 mg P L^{-1}, and mid-pond concentrations decreased from 0.07 ± 0.02 to 0.03 ± 0.01 mg P L^{-1}. In the LP, inflow concentration dropped from 0.07 ± 0.01 to 0.03 ± 0.01 mg P L^{-1}, and mid-pond from 0.06 ± 0.0 to 0.02 ± 0.00 mg P L^{-1}.

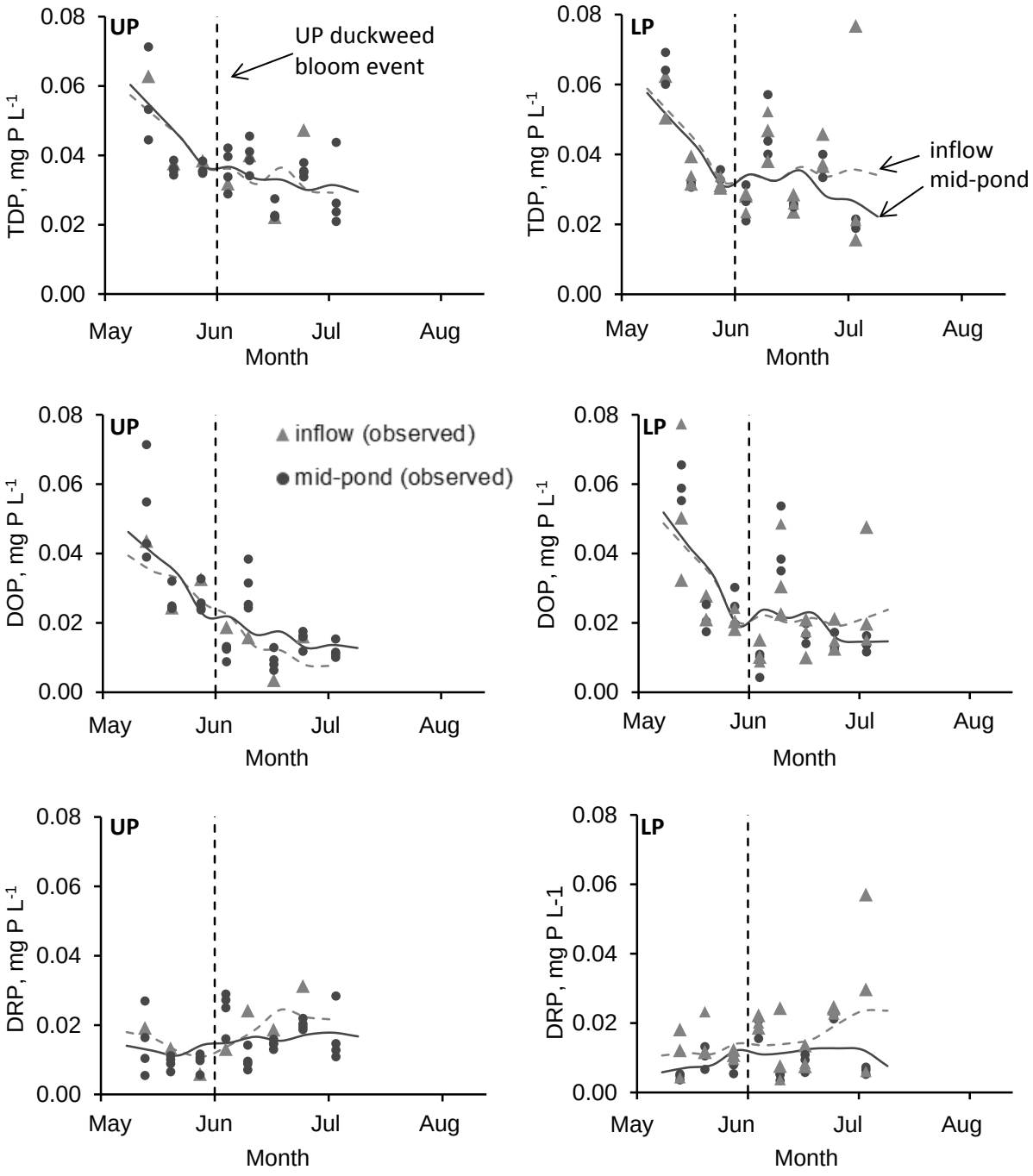

Fig. 4.5. Time trends for DRP and DOP, from 08 May - 04 July. IDW trend-line predictions are shown as lines.

As most of the TDP was in the form of DOP, it is unsurprising that DOP had a similar time trend as TDP (Fig. 4.5). Nearly all the dissolved P was in the form of DOP, and concentrations dropped steadily through the study period. In the UP, DOP concentrations dropped from 0.04 mg P L^{-1} to below detection limit (0.002 mg P L^{-1}) at both the inflow and mid-pond sites In the LP, DOP concentrations had similar dynamics, and dropped from 0.06 mg P L^{-1} to below detection limit (0.002 mg P L^{-1}) at both inflow and mid-pond sites.

DRP concentrations were low in both ponds until the end of July in the LP (Fig. 4.5). The LS means analysis indicated that DRP was higher at the UP*inflow after the DGE, but was not significantly different at any other locations (Table 4.7). DRP is the only readily bioavailable form of P for primary producers, and it has been shown that phytoplankton can quickly and efficiently eliminate DRP in small shallow systems, and control the entire regime of short-term P retention due to their capacity for rapid P uptake (Reinhardt *et al.*, 2005).

It was expected that the UP would have a rapid DGE due to increased P available for the UP, as it received surface runoff and subsurface flow from the only farm field that was treated with inorganic phosphorus fertilizer in 2014 (Table 3.1). DRP loaded into the UP would have fueled the rapid growth of duckweed, and any water that did move from the UP to the LP would have had low concentrations of DRP. Though DRP concentrations in the two ponds were not significantly different before the DGE, PP was higher and there was more flow into the ponds in May (Fig. 3.4), suggesting that nutrient loading was occurring in the short-term.

Table 4.7. Significance groupings and LS means analysis of TDP, DRP, and DOP. LS means are ordered from high to low.

Parameter	Time	Pond	Location	LS means (mg P L^{-1})	SE* (mg P L^{-1})	Groupings	
TDP	Before	UP	mid-pond	0.05	0.00	A	
	Before	UP	inflow	0.05	0.01	A	
	Before	LP	inflow	0.04	0.00	A	
	Before	LP	mid-pond	0.04	0.00	A	
	After	LP	inflow	0.04	0.00	A	
	After	UP	inflow	0.04	0.01	A	
	After	LP	mid-pond	0.04	0.00	A	
	After	UP	mid-pond	0.03	0.00	A	
DRP	After	UP	inflow	0.02	0.00		B
	After	UP	mid-pond	0.01	0.00	A	B
	After	LP	inflow	0.01	0.00	A	B
	Before	UP	inflow	0.01	0.00	A	B
	After	LP	mid-pond	0.01	0.00	A	
	Before	UP	mid-pond	0.01	0.00	A	
	Before	LP	inflow	0.01	0.00	A	
	Before	LP	mid-pond	0.01	0.00	A	
DOP	Before	LP	mid-pond	0.04	0.00	A	
	Before	UP	mid-pond	0.03	0.00	A	
	Before	LP	inflow	0.03	0.00	A	
	Before	UP	inflow	0.03	0.01	A	
	After	LP	mid-pond	0.02	0.00	A	
	After	LP	inflow	0.02	0.00	A	
	After	UP	mid-pond	0.02	0.00	A	
	After	UP	inflow	0.01	0.01	A	

* standard error.

In the LP, the eventual growth of duckweed was not the result of external loading but of internal mechanisms. The time trends and LS means indicate an increase in DRP and PP at inflows. All drainage inflows had dried out by 04 July and there had been no precipitation events for ten days prior to the final sampling day (Fig. 3.3), so it is unlikely to have been caused by DRP loaded in from runoff or the subsurface drain flows. A more likely mechanism for P increase is the

proximity of LP inflow measurements to the sediment layer. All of the LP inflows are located around the shallow edges of the pond, and measurements were taken close to the sediment layer. The increase of DRP and PP was driven by late-summer sedimentary P-release, and may have induced late-summer duckweed growth.

In shallow freshwater systems, P-release from inorganic nutrient cycling mostly occurs in the sediment and sediment-water interface (Pace and Prairie, 2005). Inorganic P is often found bound to iron (III) oxide in freshwater, which is an insoluble form of iron that is precipitated into the sediment. However, under anoxic and reducing conditions, iron (III) oxide is reduced to iron (II) oxide which causes a release of iron-bound P from the sediments into the water column (Mortimer, 1941). The steady decline in dissolved oxygen, higher concentrations of DRP, little to no discharge and flow into the LP, as well as high pH levels (Gao *et al.*, 2012) at the inflows indicate that P was being slowly released from the sediment and being made available to macrophytes as conditions became more anoxic at the sediment-water interface. This trend may have continued throughout July and led to the increased presence of duckweed in the LP.

4.3. Spatial analysis

Spatial analysis was completed on each parameter for both sampling events (Fig. 4.6) with Nugget and sill parameters noted in Table 4.8. The positive nugget of all the semivariogram models produced during kriging interpolation can be attributed to the variability arising from changing concentrations of parameters during the sampling period, as well as to measurement error (Table 4.8, Table 4.9). Example semivariograms are presented for pH mapping events in the LP (Fig. 4.7), in section 4.3.2.

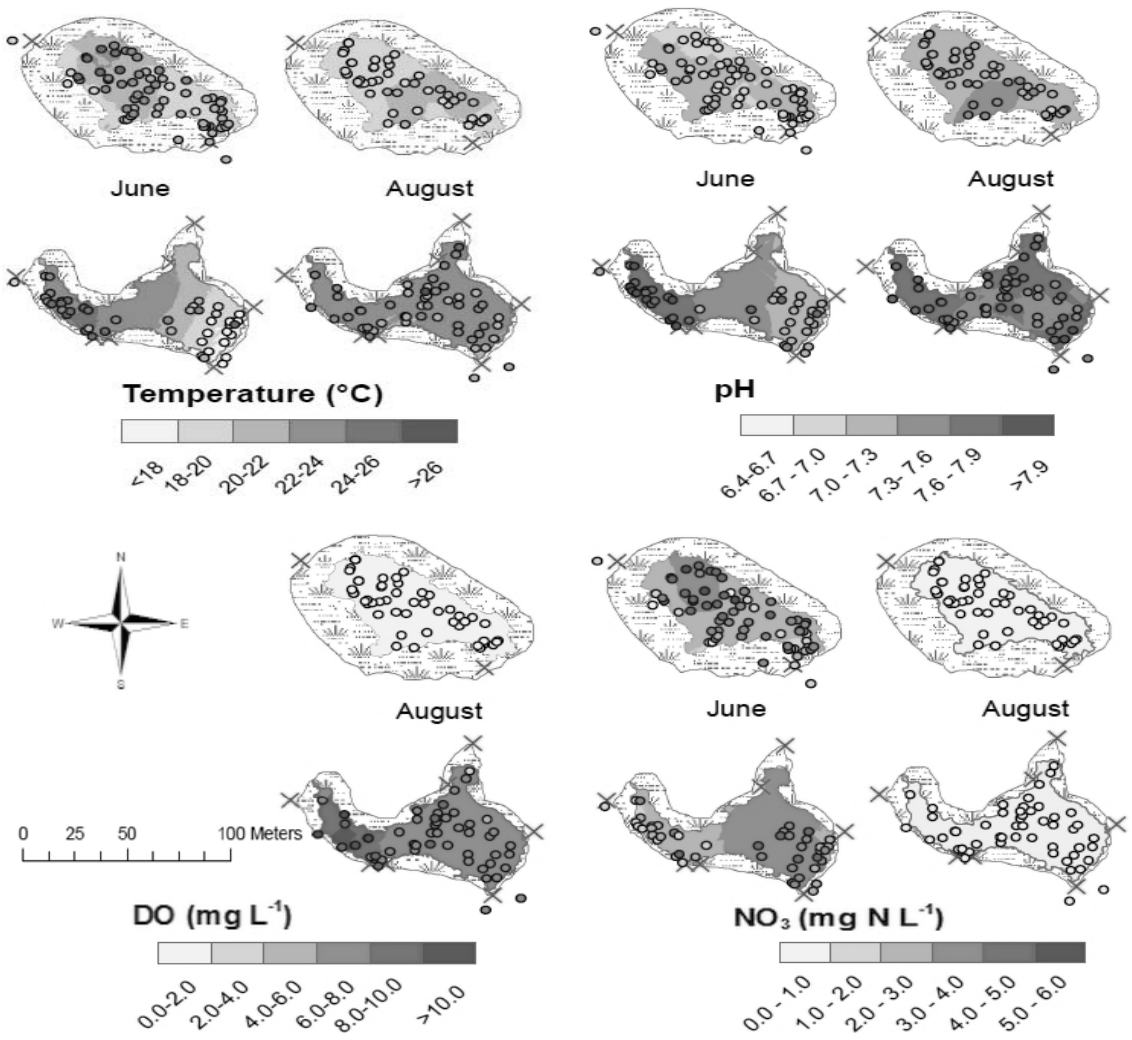

Fig 4.6. Spatial predictions of temperature, pH, dissolved oxygen, and NO_3^--N during two dense sampling events. The upper pond (UP) is displayed above the lower pond (LP) for each sampling event and predicted parameter.

4.3.1. Temperature

Kriging interpolation of the grid sampling was completed, and revealed that the pond temperature was variable in June, but relatively homogeneous in August (Fig. 4.6). In the UP in June T was consistently between 18-22 ^oC but had two distinct areas of temperature likely related to pond bathymetry. In the LP, temperatures varied in June, ranging from 18 ^oC at the East edge to greater than 26 ^oC at the West edge. In August in the LP, T was between 22-24 ^oC throughout the pond. T mapping closely predicted values at the 12 buoy locations ('x' marks on Fig. 4.1).

The semivariogram parameters attest to strong spatial dependence for T in June, with nugget:sill ratios of 0.10 and 0.16 for the UP and LP, respectively (Table 4.8). The nugget:sill ratio increased in the UP to 0.76 in August, and was unavailable in the LP due to a sill of zero, attributed to a lack of spatial structure. This suggests that spatial dependence was reduced throughout the summer for temperature, which can be seen in the homogeneity of the maps in August.

Table 4.8. Semivariogram parameters for spatial grid sensing events of dissolved oxygen, temperature, and pH

	Dissolved Oxygen				**Temperature**				**pH**			
	Range	Nugget	Sill[†]	N/S[††]	Range	Nugget	Sill[†]	N/S[††]	Range	Nugget	Sill[†]	N/S[††]
June												
UP	N/A[*]	N/A[*]	N/A[*]	N/A[*]	4.98	0.091	0.93	0.10	3.6	0.0	0.01	0.0
LP	N/A[*]	N/A[*]	N/A[*]	N/A[*]	94.55	2.95	18.7	0.16	83.92	0.033	0.24	0.14
Aug.												
UP	[**]	[**]	[**]	[**]	3.9	0.23	0.30	0.76	36.65	0.006	0.01	0.60
LP	8.05	0.410	0.6	0.68	102.7	1.36	0	N/A	6.28	0.003	0.012	0.25

[†] Partial Sill.

[††] Nugget/Sill.

[*] Data unavailable due to sensor calibration error.

[**] No spatial structure due to all concentrations below detection limit. All DO values were measured as 0.0 mg L^{-1} in the August UP sampling event.

4.3.2. pH

In the UP, pH had slight but significant spatial dynamics, remaining between 6.7-7.3 in June and 7.0-7.6 in August. pH had a wider range in the LP – during the June event, pH ranged from greater than 7.9 to between 7.0-7.3, decreasing from West to East (the direction of flow). In August, pH ranged from 7.3-7.9, with higher pH at inflows and the edges of the pond. As was the case for temperature, the semivariogram parameters for pH attest to strong spatial

dependence in June, with Nugget/sill ratios of 0.0 and 0.14 for the UP and LP, respectively (Table 4.8). The Nugget/sill ratio increased in the UP to 0.60 and 0.25 in the LP in August, indicating reduced spatial dependence of pH over time. The reduced spatial dependence of pH is striking in the semivariogram structures, which show that the sill was greatly reduced in the August mapping event (Fig 4.7).

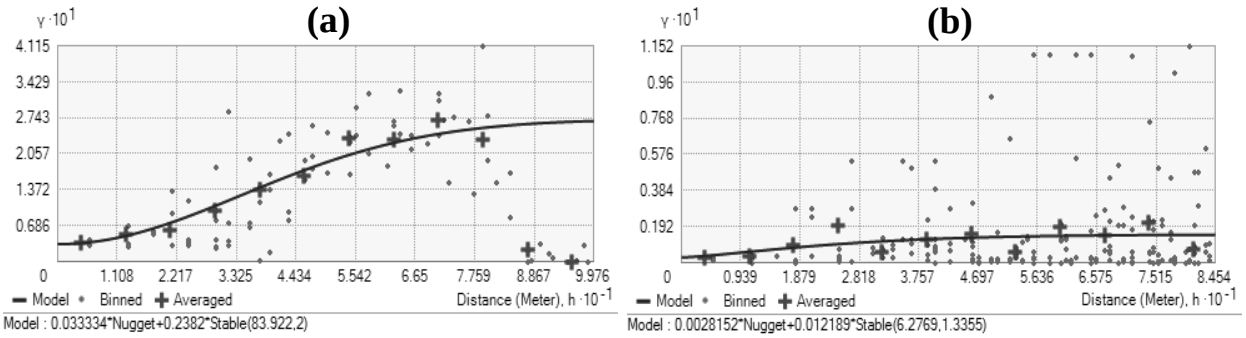

Fig. 4.7. Semivariogram models for LP mapping events in (a) June and (b) August.

Duckweed stabilizes and lowers pH beneath it due to the inhibition of photosynthetic activity within the water column and reductions in gas-exchange (Brix, 1994). This led to reduced spatial dependence in both ponds, with a more pronounced reduction in the UP. In the UP, pH was low and did not vary spatially in either mapping event. By contrast, pH in the LP where duckweed did not cover the pond exhibited more pronounced spatial patterns – especially evident in the August event in which pH is higher near inflows and around the edges of the pond. The high pH attests to photosynthetically active areas where gas exchange could occur, and where nutrients are loaded into the pond (Zimmo, 2003).

The pH maps indicate that in the UP, 1-2 sampling locations could effectively capture the spatial pH dynamics in the pond. By comparison, the LP is more spatially heterogeneous and based on the two mapping events would require up to five sampling locations to capture the pH spatial

dynamics completely, necessitating sampling points placed at the inflows and in the middle of the pond.

4.3.3. Dissolved Oxygen

In the UP, DO concentration was measured as 0.0 mg L^{-1} at all points and there was no spatial structure (Fig. 4.6). In the LP, DO concentrations ranged from greater than 6.0-10.0 mg L^{-1}. The higher DO concentrations were at the West edge of the pond, where water from the UP entered and where duckweed had not covered the surface. By August, duckweed had covered approximately 60% of the LP, largely at the North and East edges and spreading into the middle of the pond. Spatial mapping performed well in predicting concentrations at all buoy locations (see x's on Fig. 4.1). Despite a relatively high Nugget/sill ratio (0.67) suggesting weak spatial dependence for DO, there are two key areas in the LP in August with different DO concentrations – one large and less oxygenated area in the main body of the water, and one highly oxygenated area near two of the inflow locations. Based on this map, two sampling points placed in the centers of these areas would be adequate for capturing the spatial heterogeneity of DO in the LP. In the UP – after the duckweed onset – one sampling location would be adequate.

4.3.4. NO_3^--N

In both ponds, NO_3^--N activity was high in June and greatly reduced in August. In the UP in June there was higher NO_3^--N activity near the inflow location, ranging from 3.0-4.0 mg N L^{-1} as compared to the rest of the pond, where values ranged from 2.0-3.0 mg N L^{-1}. In the LP in June, there were higher concentrations towards the outlet and East side of the pond (from 3.0-4.0 mg N L^{-1}) and lower concentrations (2.0-3.0 mg N L^{-1}) at the West side of the pond, where water from the UP was entering via a culvert. In both ponds in August, NO_3^--N activity was <1.0 mg N L^{-1}.

The semivariogram parameters for NO_3^--N attest to moderate spatial dependence in June with nugget:sill ratios in of 0.44 and 0.63 for the UP and LP, respectively (Table 4.9). The ratio rose in August for the UP to 0.60 and fell in the LP to 0.0. However, the reduced nugget:sill ratio in the LP is likely a result of a lack of spatial dependence rather than the presence of it, as mapping illustrated that NO_3^--N activity was consistently below 1.0 mg N L^{-1} in August.

Table 4.9. Semivariogram parameters for spatial grid sensing events of NO_3^--N.

	NO_3^--N			
	Range	Nugget	Sill†	N/S††
June				
UP	56.90	0.15	0.34	0.44
LP	64.41	0.46	0.73	0.63
August				
UP	40.88	0.0003	0.0005	0.60
LP	6.28	0.0002	0.0002	0.0

† Partial Sill.
††Nugget/Sill.

As the outputs for both ponds dried out by 04 July, the NO_3^--N in the ponds either underwent denitrification and was reduced to a gaseous form, or was taken up by macrophytes. In the June mapping event, it was expected that higher concentrations of NO_3^--N would occur closer to the inflow loading sites of the system – especially in the UP where the time trends indicate higher input concentrations. Despite a higher concentration of NO_3^--N closer to the input, overall there was a lack of strong spatial structure for NO_3^--N in the pond. It is likely that the NO_3^--N rich water loaded from the input was immediately diffused and taken up by the duckweed in the small pond. The input is also separated from the pond water by a 5-m buffer of emergent aquatic vegetation, and water within that buffer was not mapped as it was inaccessible by boat – thus, the

water nearer to the inflow was not mapped. It is likely that the NO_3^--N was higher there, and measuring it would have shown more spatial structure in this pond.

Spatial mapping adequately predicted concentrations at all buoy locations (see 'x' marks on Fig. 4.1). Based on these results, two sampling locations for each pond would be adequate for capturing spatial dynamics of dissolved NO_3^--N.

5. Summary and Conclusions

Based on the study completed, the following conclusions were drawn:

1. The rapid onset of duckweed is driven by a combination of factors including pond depth and increased bio-available P. Duckweed cover can dramatically reduce spatial structure of pH, NO_3^--N, and DO.
2. Within a summer, dissolved inorganic fractions of nitrogen, particulate phosphorus, dissolved oxygen, and pH were shown to significantly vary in space and time. Dissolved forms of P did change through time, but proximity to inflow sites did not change concentrations and dynamics, likely due to low initial concentrations at inputs and rapid uptake by macrophytes and phytoplankton.
3. Dense spatial mapping of NO_3^--N, DO, T, and pH can be used to determine representative sampling locations for temporal monitoring schemes that capture spatial variability with the fewest number of points by defining the locations likely to represent the range of concentration or values for a target parameter. A combined use of maps – especially pH and DO – can indicate nutrient loading sites. However, manual sampling is not a practical method for collecting water quality samples at high spatial resolution; emphasis must be placed on automated sensing platforms that can take measurements more quickly and can reach hard-to-sample areas.

6. List of References

Amirbahman, A., Lake, B.A., and Norton, S.A. (2012). Seasonal phosphorus dynamics in the surficial sediment of two shallow temperate lakes: a solid-phase and pore-water study. Hydrobiologia *701*, 65–77.

Arheimer, B., and Lidén, R. (2000). Nitrogen and phosphorus concentrations from agricultural catchments—influence of spatial and time variables. Journal of Hydrology *227*, 140–159.

Aylward, B., Bandyopadhyay, J., Belausteguigotia, J., Borkey, P., Cassar, A., Meadors, L., Saade, L., Siebentritt, M., Stein, R., Tognetti, S., Tortajada, C., Allan, T., Bauer, C., Guimaraes-Pereira, A., Kendall, M., Kiersch, B., Landry, C., Mestre Rodriguez, E., Meinzen-Dick, R., Moellendorg, S., Pagiola, S., Porras, I., Ratner, B., Shea, A., Swallow, B., Thomich, T., Voutchkov, N. (2005). Freshwater ecosystem services. In Ecosystems and Human Well-Being: Policy Responses,*3*, Chopra K, Leemans R, Kumar P, Simons H (eds). Island: Washington, DC; 213–255.

Baker, L.A. (1992). Introduction to nonpoint source pollution in the United States and prospects for wetland use. Ecological Engineering *1*, 1–26.

Beauchemin, S., and Simard, R.R. (2000). Phosphorus Status of Intensively Cropped Soils of the St. Lawrence Lowlands. Soil Science Society of America Journal *64*, 659.

Becker, R.H., Sultan, M.I., Boyer, G.L., Twiss, M.R., and Konopko, E. (2009). Mapping cyanobacterial blooms in the Great Lakes using MODIS. Journal of Great Lakes Research *35*, 447–453.

Bennett, E.M., Carpenter, S.R., and Caraco, N.F. (2001). Human Impact on Erodable Phosphorus and Eutrophication: A Global Perspective Increasing accumulation of phosphorus in soil threatens rivers, lakes, and coastal oceans with eutrophication. BioScience *51*, 227–234.

Bierman, P., Lewis, M., Ostendorf, B., and Tanner, J. (2011). A review of methods for analysing spatial and time patterns in coastal water quality. Ecological Indicators *11*, 103–114.

Bjerklie, D.M., Lawrence Dingman, S., Vorosmarty, C.J., Bolster, C.H., and Congalton, R.G. (2003). Evaluating the potential for measuring river discharge from space. Journal of Hydrology *278*, 17–38.

Bonachela, S., Acuña, R.A., and Casas, J. (2007). Environmental factors and management practices controlling oxygen dynamics in agricultural irrigation ponds in a semiarid Mediterranean region: Implications for pond agricultural functions. Water Research *41*, 1225–1234.

Boström, B., Persson, G., and Broberg, B. (1988). Bioavailability of different phosphorus forms in freshwater systems. Hydrobiologia *170*, 133–155.

Braskerud, B.C. (2001). The Influence of Vegetation on Sedimentation and Resuspension of Soil Particles in Small Constructed Wetlands. Journal of Environment Quality *30*, 1447.

Brix, H. (1994). Functions of macrophytes in constructed wetlands. Water Science and Technology (United Kingdom).

Buck, O., Niyogi, D.K., and Townsend, C.R. (2004). Scale-dependence of land use effects on water quality of streams in agricultural catchments. Environmental Pollution *130*, 287–299.

Budd, J.W., and Warrington, D.S. (2004). Satellite-based Sediment and Chlorophyll a Estimates for Lake Superior. Journal of Great Lakes Research *30, Supplement 1*, 459–466.

Burgin, A.J., Hamilton, S.K., Jones, S.E., and Lennon, J.T. (2012). Denitrification by sulfur-oxidizing bacteria in a eutrophic lake. Aquat. Microb. Ecol. *66*, 283–293.

Carmichael, W.W. (2001). Health effects of toxin-producing cyanobacteria: "The CyanoHABs." Hum. Ecol. Risk Assess. *7*, 1393–1407.

Caron, D.A., Stauffer, B., Moorthi, S., Singh, A., Batalin, M., Graham, E.A., Hansen, M., Kaiser, W.J., Das, J., Pereira, A., *et al.* (2008). Macro- to fine-scale spatial and time distributions and dynamics of phytoplankton and their environmental driving forces in a small montane lake in southern California, USA. Limnol. Oceanogr. *53*, 2333–2349.

Carpenter, S.R., Caraco, N.F., Correll, D.L., Howarth, R.W., Sharpley, A.N., and Smith, V.H. (1998). Nonpoint pollution of surface waters with phosphorus and nitrogen. Ecological Applications *8*, 559–568.

Casado, M.R., Gonzalez, R.B., Kriechbaumer, T., and Veal, A. (2015). Automated Identification of River Hydromorphological Features Using UAV High Resolution Aerial Imagery. Sensors *15*, 27969–27989.

Casper, A.F., Dixon, B., Steimle, E.T., Hall, M.L., and Conmy, R.N. (2012). Scales of heterogeneity of water quality in rivers: Insights from high resolution maps based on integrated geospatial, sensor and ROV technologies. Applied Geography *32*, 455–464.

Causse, J., Baures, E., Mery, Y., Jung, A.-V., and Thomas, O. (2015). Variability of N Export in Water: A Review. Crit. Rev. Environ. Sci. Technol. *45*, 2245–2281.

Chambers, P.A., McGoldrick, D.J., Brua, R.B., Vis, C., Culp, J.M., and Benoy, G.A. (2012). Development of Environmental Thresholds for Nitrogen and Phosphorus in Streams. J. Environ. Qual. *41*, 7–20.

Chen, M., Ye, T.-R., Krumholz, L.R., and Jiang, H.-L. (2014). Temperature and Cyanobacterial Bloom Biomass Influence Phosphorous Cycling in Eutrophic Lake Sediments. PLoS One *9*.

Chipman, J.W., Lillesand, T.M., Schmaltz, J.E., Leale, J.E., and Nordheim, M.J. (2004). Mapping lake water clarity with Landsat images in Wisconsin, U.S.A. Canadian Journal of Remote Sensing *30*, 1–7.

Cooper, D.M. (2004). Some effects of sampling design on water quality estimation in streams. Hydrol. Sci. J.-J. Sci. Hydrol. *49*, 1055–1080.

Cornwell, J.C., Kemp, W.M., and Kana, T.M. (1999). Denitrification in coastal ecosystems: methods, environmental controls, and ecosystem level controls, a review. Aquatic Ecology *33*, 41–54.

Dale, H.M., and Gillespie, T. (1976). The influence of floating vascular plants on the diurnal fluctuations of temperature near the water surface in early spring. Hydrobiologia *49*, 245–256.

Davies, J.-M., and Mazumder, A. (2003). Health and environmental policy issues in Canada: the role of watershed management in sustaining clean drinking water quality at surface sources. J. Environ. Manage. *68*, 273–286.

DeBell, L., Anderson, K., Brazier, R.E., King, N., and Jones, L. (2015). Water resource management at catchment scales using lightweight UAVs: current capabilities and future perspectives. J. Unmanned Veh. Sys. 1–24.

Deitchmann, R. (2009). Thermal remote sensing of stream temperature and groundwater discharge: Applications to hydrogeology and water resources policy in the state of Wisconsin. M.Sc. Thesis. University of Wisconsin-Madison.

De Jong, R., Drury, C.F., Yang, J.Y., and Campbell, C.A. (2009). Risk of water contamination by nitrogen in Canada as estimated by the IROWC-N model. Journal of Environmental Management *90*, 3169–3181.

Dekker, A.G., Vos, R.J., and Peters, S.W.M. (2002). Analytical algorithms for lake water TSM estimation for retrospective analyses of TM and SPOT sensor data. International Journal of Remote Sensing *23*, 15–35.

Dolliver, H., and Gupta, S. (2008). Antibiotic Losses in Leaching and Surface Runoff from Manure-Amended Agricultural Land. Journal of Environment Quality *37*, 1227.

Downing, J.A., Prairie, Y.T., Cole, J.J., Duarte, C.M., Tranvik, L.J., Striegl, R.G., McDowell, W.H., Kortelainen, P., Caraco, N.F., Melack, J.M., *et al.* (2006). The global abundance and size distribution of lakes, ponds, and impoundments. Limnol. Oceanogr. *51*, 2388–2397.

Dunbabin, M., and Grinham, A. (2010). Experimental evaluation of an Autonomous Surface Vehicle for water quality and greenhouse gas emission monitoring. In 2010 IEEE International Conference on Robotics and Automation (ICRA), pp. 5268–5274.

Dutilleul, P. (2011). Spatio-Temporal Heterogeneity: Concepts and Analyses (Cambridge University Press).

Eastman, M. (2008). Field-scale nutrient transport monitoring and modeling of subsurface and naturally drained agricultural lands. M.Sc. Thesis. Dept. of Bioresource Engineering, McGill University.

Ellison, R., and Slocum, D. (2008). High spatial resolution mapping of water quality and bathymetry with a person-deployable, low cost autonomous underwater vehicle. In OCEANS 2008, pp. 1–7.

ElSayed, E.M., Prasher, S.O., and Patel, R.M. (2013). Effect of nonionic surfactant Brij 35 on the fate and transport of oxytetracycline antibiotic in soil. Journal of Environmental Management *116*, 125–134.

Evans, D.J., and Johnes, P.J. (2004). Physico-chemical controls on phosphorus cycling in two lowland streams. Part 1 – the water column. Science of The Total Environment *329*, 145–163.

Falkowski, P., Scholes, R.J., Boyle, E., Canadell, J., Canfield, D., Elser, J., Gruber, N., Hibbard, K., Hogberg, P., Linder, S., *et al.* (2000). The global carbon cycle: A test of our knowledge of earth as a system. Science *290*, 291–296.

Fingas, M., and Brown, C. (2014). Review of oil spill remote sensing. Marine Pollution Bulletin *83*, 9–23.

Flynn, K.F., and Chapra, S.C. (2014). Remote Sensing of Submerged Aquatic Vegetation in a Shallow Non-Turbid River Using an Unmanned Aerial Vehicle. Remote Sensing *6*, 12815–12836.

Gächter, R., and Meyer, J.S. (1993). The role of microorganisms in mobilization and fixation of phosphorus in sediments. In Proceedings of the Third International Workshop on Phosphorus in Sediments, P.C.M. Boers, T.E. Cappenberg, and W. van Raaphorst, eds. (Springer Netherlands), pp. 103–121.

Galvez-Cloutier, R., and Sanchez, M. (2007). Trophic Status Evaluation for 154 Lakes in Quebec, Canada: Monitoring and Recommendations. Water Qual. Res. J. Canada *42*, 252–268.

Gao, Y., Cornwell, J.C., Stoecker, D.K., and Owens, M.S. (2012). Effects of cyanobacterial-driven pH increases on sediment nutrient fluxes and coupled nitrification-denitrification in a shallow fresh water estuary. Biogeosciences *9*, 2697–2710.

Garcia-Cordova, F., and Guerrero-Gonzalez, A. (2013). Intelligent Navigation for a Solar Powered Unmanned Underwater Vehicle. Int. J. Adv. Robot. Syst. *10*, 185.

Glasgow, H.B., Burkholder, J.M., Reed, R.E., Lewitus, A.J., and Kleinman, J.E. (2004). Real-time remote monitoring of water quality: a review of current applications, and advancements in sensor, telemetry, and computing technologies. Journal of Experimental Marine Biology and Ecology *300*, 409–448.

Gollamudi, A., Madramootoo, C.A., and Enright, P. (2007). Water quality modeling of two agricultural fields in southern Quebec using SWAT. Trans. ASABE *50*, 1973–1980.

Gómez, J.A.D., Alonso, C.A., and García, A.A. (2011). Remote sensing as a tool for monitoring water quality parameters for Mediterranean Lakes of European Union water framework directive (WFD) and as a system of surveillance of cyanobacterial harmful algae blooms (SCyanoHABs). Environ Monit Assess *181*, 317–334.

Graham, S. (1999). Remote Sensing. Retrieved from NASA website: http://earthobservatory.nasa.gov/Features/RemoteSensing/remote_08.php

Gruijter, J. de, Brus, D.J., Bierkens, M.F.P., and Knotters, M. (2006). Sampling for Natural Resource Monitoring (Springer Science & Business Media).

Hains, J.J., and Kennedy, R.H. (2002). Rapid Collection of Spatially-Explicit In-Situ Water Quality Data Using a Programmable Towed Vehicle. Journal of Freshwater Ecology *17*, 99–107.

Han, L., and Jordan, K.J. (2005). Estimating and mapping chlorophyll-a concentration in Pensacola Bay, Florida using Landsat ETM+ data. International Journal of Remote Sensing *26*, 5245–5254.

He, Z.L., Zhang, M.K., Calvert, D.V., Stoffella, P.J., Yang, X.E., and Yu, S. (2004). Transport of Heavy Metals in Surface Runoff from Vegetable and Citrus Fields. Soil Science Society of America Journal *68*, 1662.

Hecky, R.E., and Kilham, P. (1988). Nutrient limitation of phytoplankton in freshwater and marine environments: A review of recent evidence on the effects of enrichment1. Limnol. Oceanogr. *33*, 796–822.

Heini, A., Puustinen, I., Tikka, M., Jokiniemi, A., Leppäranta, M., and Arvola, L. (2014). Strong dependence between phytoplankton and water chemistry in a large temperate lake: spatial and time perspective. Hydrobiologia *731*, 139–150.

Hestir, E.L., Brando, V.E., Bresciani, M., Giardino, C., Matta, E., Villa, P., and Dekker, A.G. (2015). Measuring freshwater aquatic ecosystems: The need for a hyperspectral global mapping satellite mission. Remote Sensing of Environment *167*, 181–195.

Hillman, W.S. (1961). The Lemnaceae, or duckweeds. Bot. Rev *27*, 221–287.

Holtan, H., Kamp-Nielsen, L., and Stuanes, A.O. (1988). Phosphorus in Soil, Water and Sediment: An Overview. In Phosphorus in Freshwater Ecosystems, G. Persson, and M. Jansson, eds. (Springer Netherlands), pp. 19–34.

House, W.A. (2003). Geochemical cycling of phosphorus in rivers. Applied Geochemistry *18*, 739–748.

Howarth, R.W., Marino, R., and Cole, J.J. (1988). Nitrogen fixation in freshwater, estuarine, and marine ecosystems. 2. Biogeochemical controls1. Limnol. Oceanogr. *33*, 688–701.

Huang, J., Gao, J., Hörmann, G., and Fohrer, N. (2014). Modeling the effects of environmental variables on short-term spatial changes in phytoplankton biomass in a large shallow lake, Lake Taihu. Environ Earth Sci *72*, 3609–3621.

Hudnell, H.K. (2010). The state of U.S. freshwater harmful algal blooms assessments, policy and legislation. Toxicon *55*, 1024–1034.

Huntsberger, T., and Woodward, G. (2011). Intelligent autonomy for unmanned surface and underwater vehicles. In OCEANS 2011, pp. 1–10.

Hupfer, M., and Lewandowski, J. (2008). Oxygen Controls the Phosphorus Release from Lake Sediments – a Long-Lasting Paradigm in Limnology. International Review of Hydrobiology *93*, 415–432.

Husson, E., Hagner, O., and Ecke, F. (2014). Unmanned aircraft systems help to map aquatic vegetation. Appl Veg Sci *17*, 567–577.

IRDA. (1970). Digital Soil Survey Report, 1:20 000. Sainte-Foy: Institut de recherche et de développement en agroenvironnement Inc.

ISO. (1980). Water flow measurement in open channels using weirs and venturi flumes - Part 1: Thin plate weirs. International Organization of Standards. ISO 1438/1-1980(E).

Jamieson, A., Madramootoo, C.A., and Enright, P. (2003). Phosphorus losses in surface and subsurface runoff from a snowmelt event on an agricultural field in Quebec. Canadian Biosystems Engineering = Le Genie Des Biosystemes Au Canada : La Revue de La Societe Canadienne de Genie Agroalimentaire et Biologique.

Jarvie, H.P., Sharpley, A.N., Withers, P.J.A., Scott, J.T., Haggard, B.E., and Neal, C. (2013). Phosphorus Mitigation to Control River Eutrophication: Murky Waters, Inconvenient Truths, and "Postnormal" Science. J. Environ. Qual. *42*, 295–304.

Johnes, P.J., and Burt, T.P. (1993). Nitrate in surface waters. 269–317.

van Kessel, C., Clough, T., and van Groenigen, J.W. (2009). Dissolved Organic Nitrogen: An Overlooked Pathway of Nitrogen Loss from Agricultural Systems? Journal of Environment Quality *38*, 393.

Kotchi, S.O., Brazeau, S., Turgeon, P., Pelcat, Y., Legare, J., Lavigne, M.-P., Essono, F.N., Fournier, R.A., and Michel, P. (2015). Evaluation of Earth Observation Systems for Estimating Environmental Determinants of Microbial Contamination in Recreational Waters. IEEE J. Sel. Top. Appl. Earth Observ. Remote Sens. *8*, 3730–3741.

Kovacic, D.A., David, M.B., Gentry, L.E., Starks, K.M., and Cooke, R.A. (2000). Effectiveness of constructed wetlands in reducing nitrogen and phosphorus export from agricultural tile drainage. J. Environ. Qual. *29*, 1262–1274.

Kumar, M., and Lin, J.-G. (2010). Co-existence of anammox and denitrification for simultaneous nitrogen and carbon removal—Strategies and issues. Journal of Hazardous Materials *178*, 1–9.

Lega, M., Kosmatka, J., Ferrara, C., Russo, F., Napoli, R.M.A., and Persechino, G. (2012). Using Advanced Aerial Platforms and Infrared Thermography to Track Environmental Contamination. Environmental Forensics *13*, 332–338.

Li, Y.P., Tang, C.Y., Yu, Z.B., and Acharya, K. (2014). Correlations between algae and water quality: factors driving eutrophication in Lake Taihu, China. International Journal of Environmental Science and Technology : (IJEST) *11*, 169–182.

Liang, B.C., and MacKenzie, A.F. (1994). Corn yield, nitrogen uptake and nitrogen use efficiency as influenced by nitrogen fertilization. Can. J. Soil. Sci. *74*, 235–240.

Lim, K.J., Engel, B.A., Tang, Z., Choi, J., Kim, K.-S., Muthukrishnan, S., and Tripathy, D. (2005). Automated Web Gis Based Hydrograph Analysis Tool, What1. JAWRA Journal of the American Water Resources Association *41*, 1407–1416.

Ma, R., and Dai, J. (2005). Investigation of chlorophyll-a and total suspended matter concentrations using Landsat ETM and field spectral measurement in Taihu Lake, China. International Journal of Remote Sensing *26*, 2779–2795.

Martinuzzi, S., Januchowski-Hartley, S.R., Pracheil, B.M., McIntyre, P.B., Plantinga, A.J., Lewis, D.J., and Radeloff, V.C. (2014). Threats and opportunities for freshwater conservation under future land use change scenarios in the United States. Glob Change Biol *20*, 113–124.

Matthews, M.W., Bernard, S., and Winter, K. (2010). Remote sensing of cyanobacteria-dominant algal blooms and water quality parameters in Zeekoevlei, a small hypertrophic lake, using MERIS. Remote Sens. Environ. *114*, 2070–2087.

Mei, K., Liao, L., Zhu, Y., Lu, P., Wang, Z., Dahlgren, R.A., and Zhang, M. (2014). Evaluation of spatial-time variations and trends in surface water quality across a rural-suburban-urban interface. Environ Sci Pollut Res *21*, 8036–8051.

MINISTÈRE DU DÉVELOPPEMENT DURABLE, DE L'ENVIRONNEMENT ET DE LA LUTTE CONTRE LES CHANGEMENTS CLIMATIQUES (MDDELC) (2015). Bilan de la gestion des épisodes de fleurs d'eau d'algues bleu-vert en 2014 - Résultats pour les plans d'eau et les installations de production d'eau potable (Quebec: Direction du suivi de l'état de l'environnement).

Ministry of Environment of Quebec (2011). St. Lawrence Action Plan 2011-2026.

Moodley, K., Pillay, S., and Pather, K. (2015). Spatiotemporal characterization of water chemistry and pollution sources of the Umhlatuzana, Umbilo and Amanzimnyama River catchments of Durban, KwaZulu-Natal, South Africa. Environ Earth Sci *74*, 1273–1289.

Morris, K., Harrison, K.A., Bailey, P.C., and Boon, P.I. (2004). Domain shifts in the aquatic vegetation of shallow urban lakes: the relative roles of low light and anoxia in the catastrophic loss of the submerged angiosperm Vallisneria americana. Mar. Freshwater Res. *55*, 749–758.

Mortimer, C.H. (1942). The Exchange of Dissolved Substances between Mud and Water in Lakes. Journal of Ecology *30*, 147–201.

Moya, I., Camenen, L., Evain, S., Goulas, Y., Cerovic, Z.G., Latouche, G., Flexas, J., and Ounis, A. (2004). A new instrument for passive remote sensing: 1. Measurements of sunlight-induced chlorophyll fluorescence. Remote Sensing of Environment *91*, 186–197.

NOAA (2015). What is remote sensing? Retrieved from the National Ocean and Atmospheric Administration website: http://oceanservice.noaa.gov/facts/remotesensing.html

Novotny, V. (1999). Diffuse pollution from agriculture - A worldwide outlook. Water Sci. Technol. *39*, 1–13.

Oliver, M.A., and Webster, R. (1990). Kriging: a method of interpolation for geographical information systems. International Journal of Geographical Information Systems *4*, 313–332.

Pace, M., and Prairie, Y. (2005). Respiration in Lakes. In Respiration in Aquatic Ecosystems, (Oxford University Press, USA).

Paerl, H.W., Fulton, R.S., Moisander, P.H., and Dyble, J. (2001). Harmful Freshwater Algal Blooms, With an Emphasis on Cyanobacteria. The Scientific World Journal *1*, 76–113.

Peukert, S., Griffith, B.A., Murray, P.J., Macleod, C.J.A., and Brazier, R.E. (2014). Intensive Management in Grasslands Causes Diffuse Water Pollution at the Farm Scale. Journal of Environment Quality *43*, 2009.

Pilgrim, D.H., Cordery, I., and Baron, B.C. (1982). Effects of catchment size on runoff relationships. Journal of Hydrology *58*, 205–221.

Pratt, B., and Chang, H. (2012). Effects of land cover, topography, and built structure on seasonal water quality at multiple spatial scales. Journal of Hazardous Materials *209–210*, 48–58.

Qin, B., Zhu, G., Gao, G., Zhang, Y., Li, W., Paerl, H.W., and Carmichael, W.W. (2010). A drinking water crisis in Lake Taihu, China: linkage to climatic variability and lake management. Environ Manage *45*, 105–112.

Rabalais, N.N., Diaz, R.J., Levin, L.A., Turner, R.E., Gilbert, D., and Zhang, J. (2010). Dynamics and distribution of natural and human-caused hypoxia. Biogeosciences *7*, 585–619.

Raimondi, F.M., Trapanese, M., Franzitta, V., Viola, A., and Colucci, A. (2015). A innovative semi-immergible USV (SI-USV) drone for marine and lakes operations with instrumental telemetry and acoustic data acquisition capability. In OCEANS 2015 - Genova, pp. 1–10.

Rasouli, S., Whalen, J.K., and Madramootoo, C.A. (2014a). Review: Reducing residual soil nitrogen losses from agroecosystems for surface water protection in Quebec and Ontario, Canada: Best management practices, policies and perspectives. Can. J. Soil. Sci. *94*, 109–127.

Rasouli, S., Whalen, J.K., and Madramootoo, C.A. (2014b). Review: Reducing residual soil nitrogen losses from agroecosystems for surface water protection in Quebec and Ontario, Canada: Best management practices, policies and perspectives. Can. J. Soil. Sci. *94*, 109–127.

Reinhardt, M., Gächter, R., Wehrli, B., and Müller, B. (2005). Phosphorus Retention in Small Constructed Wetlands Treating Agricultural Drainage Water. Journal of Environment Quality *34*, 1251.

Robertson, D.M., and Roerish, E.D. (1999). Influence of various water quality sampling strategies on load estimates for small streams. Water Resour. Res. *35*, 3747–3759.

Rossel, V., A, R., McBratney, A.B., and Minasny, B. (2010). Proximal soil sensing (Springer).

Rousseau, A.N., Savary, S., Hallema, D.W., Gumiere, S.J., and Foulon, É. (2013). Modeling the effects of agricultural BMPs on sediments, nutrients, and water quality of the Beaurivage River watershed (Quebec, Canada). Canadian Water Resources Journal / Revue Canadienne Des Ressources Hydriques *38*, 99–120.

Rutherford, J.C., Blackett, S., Blackett, C., Saito, L., and Davies-Colley, R.J. (1997). Predicting the effects of shade on water temperature in small streams. New Zealand Journal of Marine and Freshwater Research *31*, 707–721.

Rysgaard, S., Risgaard-Petersen, N., Niels Peter, S., Kim, J., and Lars Peter, N. (1994). Oxygen regulation of nitrification and denitrification in sediments. Limnol. Oceanogr. *39*, 1643–1652.

Sartoris, J.J., Thullen, J.S., Barber, L.B., and Salas, D.E. (1999). Investigation of nitrogen transformations in a southern California constructed wastewater treatment wetland. Ecological Engineering *14*, 49–65.

Shapiro, J. (1997). The role of carbon dioxide in the initiation and maintenance of blue-green dominance in lakes. Freshw. Biol. *37*, 307–323.

Shrestha, S., and Kazama, F. (2007). Assessment of surface water quality using multivariate statistical techniques: A case study of the Fuji river basin, Japan. Environmental Modelling & Software *22*, 464–475.

Simard, G. (2005). Nutrient transport from agricultural fields. McGill University.

Sims, J.T., Simard, R.R., and Joern, B.C. (1998). Phosphorus loss in agricultural drainage: historical perspective and current research. Journal of Environmental Quality *27*, 277–293.

Skaggs, R.W., Youssef, A.A., Chescheir, G.M., and Gilliam, J.W. (2005). Effect of drainage intensity on nitrogen losses from drained lands. Trans. ASAE *48*, 2169–2177.

Smeltzer, E., Shambaugh, A. d., and Stangel, P. (2012). Environmental change in Lake Champlain revealed by long-term monitoring. Journal of Great Lakes Research *38*, *Supplement 1*, 6–18.

Smith, L.C., Isacks, B.L., Bloom, A.L., and Murray, A.B. (1996). Estimation of discharge from three braided rivers using synthetic aperture radar satellite imagery: Potential application to ungaged basins. Water Resources Research *32*, 2021–2034.

Smith, D.R., Owens, P.R., Leytem, A.B., and Warnemuende, E.A. (2007). Nutrient losses from manure and fertilizer applications as impacted by time to first runoff event. Environmental Pollution *147*, 131–137.

Solomon, K.R., Baker, D.B., Richards, R.P., Dixon, D.R., Klaine, S.J., LaPoint, T.W., Kendall, R.J., Weisskopf, C.P., Giddings, J.M., Giesy, J.P., *et al.* (1996). Ecological risk assessment of atrazine in North American surface waters. Environ. Toxicol. Chem. *15*, 31–74.

Song, K., Xenopoulos, M.A., Buttle, J.M., Marsalek, J., Wagner, N.D., Pick, F.R., and Frost, P.C. (2013). Thermal stratification patterns in urban ponds and their relationships with vertical nutrient gradients. Journal of Environmental Management *127*, 317–323.

Staehr, P.A., Christensen, J.P.A., Batt, R.D., and Read, J.S. (2012). Ecosystem metabolism in a stratified lake. Limnol. Oceanogr. *57*, 1317–1330.

Stutter, M.I., Langan, S.J., and Cooper, R.J. (2008). Spatial and time dynamics of stream water particulate and dissolved N, P and C forms along a catchment transect, NE Scotland. Journal of Hydrology *350*, 187–202.

Sun, B., Zhou, S., and Zhao, Q. (2003). Evaluation of spatial and temporal changes of soil quality based on geostatistical analysis in the hill region of subtropical China. Geoderma *115*, 85–99.

Teece, M.A. (2009). An inexpensive remotely operated vehicle for underwater studies. Limnol. Oceanogr. Methods *7*, 206–215.

Torbick, N., Hession, S., Hagen, S., Wiangwang, N., Becker, B., and Qi, J. (2013). Mapping inland lake water quality across the Lower Peninsula of Michigan using Landsat TM imagery. International Journal of Remote Sensing *34*, 7607–7624.

US EPA. (2012a). What is a Watershed? Retrieved from the Environmental Protection Agency website: http://water.epa.gov/type/watersheds/whatis.cfm

US EPA, (2012b). 5.7 Nitrates. Retrieved from the Environmental Protection Agency website: http://water.epa.gov/type/rsl/monitoring/vms57.cfm

US EPA, (2008). Volunteer Lake Monitoring Manual. Retrieved from the Environmental Protection Agency website: http://water.epa.gov/type/watersheds/monitoring/lakevm.cfm

US EPA, (2003). Standard Operating Procedure: Surface Water Sampling. Retrieved from the Environmental Protection Agency website: http://www2.epa.gov/region8/standard-operating-procedure-surface-water-sampling

Vance-Borland, K., Burnett, K., and Clarke, S. (2009). Influence of mapping resolution on assessments of stream and streamside conditions: lessons from coastal Oregon, USA. Aquatic Conserv: Mar. Freshw. Ecosyst. *19*, 252–263.

Vandeberg, G.S., Dixon, C.S., Vose, B., and Fisher, M.R. (2015). Spatial assessment of water quality in the vicinity of Lake Alice National Wildlife Refuge, Upper Devils Lake Basin, North Dakota. Environ Monit Assess *187*, 40.

Van der Merwe, D., and Price, K.P. (2015). Harmful Algal Bloom Characterization at Ultra-High Spatial and Time Resolution Using Small Unmanned Aircraft Systems. Toxins (Basel) *7*, 1065–1078.

Verhoeven, J.T.A., Arheimer, B., Yin, C., and Hefting, M.M. (2006). Regional and global concerns over wetlands and water quality. Trends in Ecology & Evolution *21*, 96–103.

Web of Science TOPIC: (((spatial and time) or spatiotemporal) and (watershed or catchment or drainage basin or pond* or river* or stream* or estuar* or freshwater) AND DOCUMENT TYPES: (ARTICLE) Timespan=All years.

Weiss, R.F. (1970). The solubility of nitrogen, oxygen and argon in water and seawater. Deep Sea Research and Oceanographic Abstracts *17*, 721–735.

Weyhenmeyer, G.A., Jeppesen, E., Adrian, R., Arvola, L., Blenckner, T., Jankowski, T., Jennings, E., Noges, P., Noges, T., and Straile, D. (2007). Nitrate-depleted conditions on the increase in shallow northern European lakes. Limnol. Oceanogr. *52*, 1346–1353.

Wilde, F.D. (2008). Book 9 - Handbooks for Water-Resources Investigations. In National Field Manual for the Collection of Water-Quality Data,.

Yates, C.R. (2008). Comparison of two constructed wetland substrates for reducing phosphorus and nitrogen pollution in agricultural runoff. Bioresource Engineering. Ste-Anne-De-Bellevure, Quebec, McGill University, Macdonald Campus. MSc.

Ye, R., Shan, K., Gao, H., Zhang, R., Xiong, W., Wang, Y., and Qian, X. (2014). Spatio-temporal Distribution Patterns in Environmental Factors, Chlorophyll-a and Microcystins in a Large Shallow Lake, Lake Taihu, China. Int. J. Environ. Res. Public Health *11*, 5155–5169.

Ying, G.G., Kookana, R.S., and Ru, Y.J. (2002). Occurrence and fate of hormone steroids in the environment. Environ. Int. *28*, 545–551.

Zang, W., Lin, J., Wang, Y., and Tao, H. (2012). Investigating small-scale water pollution with UAV Remote Sensing Technology. In World Automation Congress (WAC), 2012, pp. 1–4.

Zimmerman, D.L. (2006). Optimal network design for spatial prediction, covariance parameter estimation, and empirical prediction. Environmetrics *17*, 635–652.

Zimmo, O.R., van der Steen, N.P., and Gijzen, H.J. (2004). Nitrogen mass balance across pilot-scale algae and duckweed-based wastewater stabilisation ponds. Water Research *38*, 913–920.

Appendices

A. R-Code for statistical analysis of the Nested Factorial Model design

```
#Housekeeping
file.names <- dir(path, pattern ="/C:/data/all_files.csv")
libraries(LSmeans,multcompview,MASS)

# For loop to iterate through all parameters
for(i in(file.names)){
  infile <- paste("C:/Users/…/R_wd/Stats/ANOVA/",i,sep="")
  mydata <- read.csv(infile)
  names(mydata)[names(mydata)=="time"] <- "time"
#myvars is a list of all variable names
  myvars= names(mydata[5:8])

# sub-sample data for statistical comparison
  mydata <- mydata[which(mydata$Day!= "95"), ]
  mydata <- mydata[which(mydata$Day!= "28"), ]
  mydata <- mydata[which(mydata$Day!= "58"), ]
  subdata = mydata[myvars]
  subdata = na.omit(subdata)
  attach(subdata)

# Consider parameters as factors, not numerics
# “pond” var: either ‘UP’ for upper pond or’ LP’ for lower pond
  pond <- as.character(pond)
# Changing “pond” variable values from strings to a numeric  binary value
  pond[pond == "0"] <- "UP"
  pond[pond == "1"] <- "LP"
# “location” var values ‘Input’ for measurement near inputs, or ‘Mid’ in pond middle
  location <- as.character(location)
# Changing “location” variable values from strings to a numeric  binary value
  location[location == "0"] <- "Input"
  location[location == "1"] <- "Mid"
# “time” var values ‘Before’ for measurements before duckweed bloom, or ‘After’ for after
time <- as.character(time)
# Changing “time” variable values from strings to a numeric  binary value
  time[time== "0"] <- "Before"
  time[time== "1"] <- "After"
  pond = factor(pond, c("UP","LP"))
  time= factor(time, c("Before","After"))

# Model location nested in pond with threeway interaction
```

```
   Model <- glm(subdata[[1]]~pond + pond/location + time +
time*pond/location,na.action=na.omit)
   print(summary(Model))
   print(step(Model, direction="both"))
   writeLines(paste("pairwise differences using tukey's adjustment for",names(subdata[1])))
# Create var “LS.stored” to store outputs of LS means analysis on the model
   LS.stored <- LSmeans(Model, cld~time:pond:location, adjust ="scheffe")
   summary(LS.stored)
   print(LS.stored)

#print LSmeans box/whisker plot
   dev.new()
   print(plot(LS.stored,xlab=paste(c("LS means of",names(subdata[1])))))

 detach(subdata)
  rm(list=ls())
}
```

B. USV design and testing

B.1. USV system design

Water quality monitoring can be expensive, laborious, unrepresentative, and often impractical with current standard methods. This is especially true of spatially heterogeneous and difficult-to-monitor freshwater bodies such as rivers, streams, and catchments. To address these challenges, an Unmanned Surface Vehicle (USV) capable of carrying diverse sensor payloads was designed and preliminary range testing was completed. The complete system comprises: (a) ground station for data logging and user inputs for navigation, (b) a USV, and (c) a sensor platform (Fig. B-1). The construction and design of the USV was led by Dr. Luan Pan, while the construction and design of the sensor platform was led by Dr. Abdul Mannan.

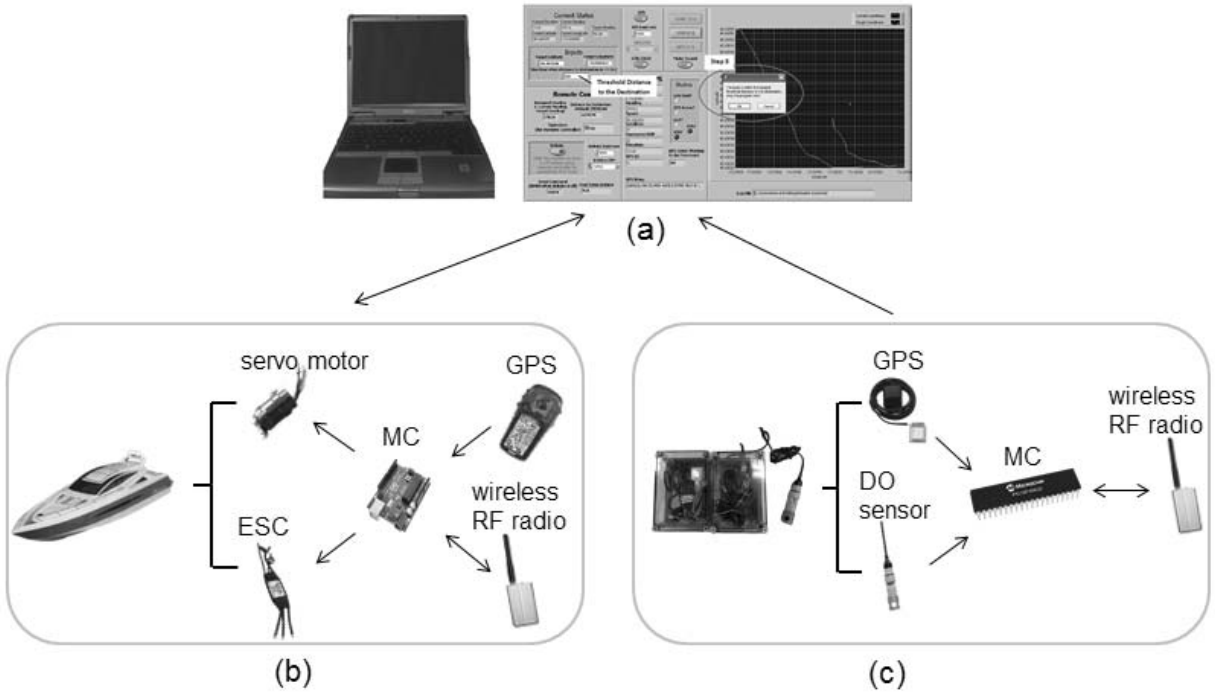

Fig. B-1. Layout of overall system depicting (a) ground station, (b) USV and components of automated navigation, and (c) sensor platform.

The USV is a retrofitted RC boat with a 125 A water-cooled Electronic Speed Controller (ESC) for thrust and a 1604 kV brushless servo motor for direction control (Fig. B-2). The vehicle is equipped with an Arduino microcontroller, handheld GPS (eTrex, Garmin Industries, Lenexa, Kansas, USA), and wireless RF radios for data and position logging. The USV is capable of manual and automated modes of operation - in manual mode, the platform is controlled via remote control; in automated mode, the platform can be instructed to automatically sample at multiple locations. Range tests indicate that the platform can operate in manual mode from up to 350 m away, and in automated mode from up to 1980 m away (limited by the communication range of the wireless RF radios).

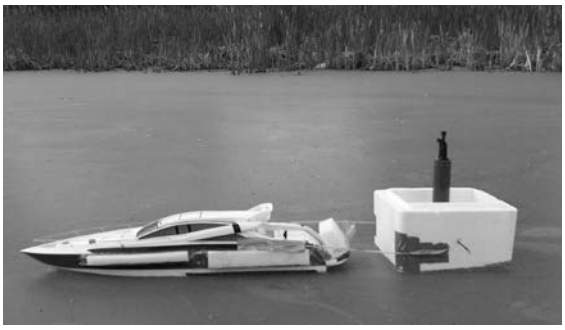

Fig. B-2. The brushless V-hull remote control boat, towing an earlier sensor platform design.

Specifications for the remote control boat:
Length: 1000 mm
Width: 300 mm
Height: 270 mm
Weight: 2.6 kg
Motor: 36-60 size 1604 kV water-cooled brushless
ESC: 125 A water-cooled

The sensor platform comprises two waterproof housing units. One unit contains a GPS module (PMB-688, Digi-Key Electronics, Thief River Falls, MN, USA) and a PIC (18F45K22, Digi-Key Electronics, Thief River Falls, MN, USA) microcontroller-based circuit for the measurement of dissolved oxygen (Fig. B-3). The other unit contains a power supply and wireless RF radio that sends sensor and GPS data to the ground station.

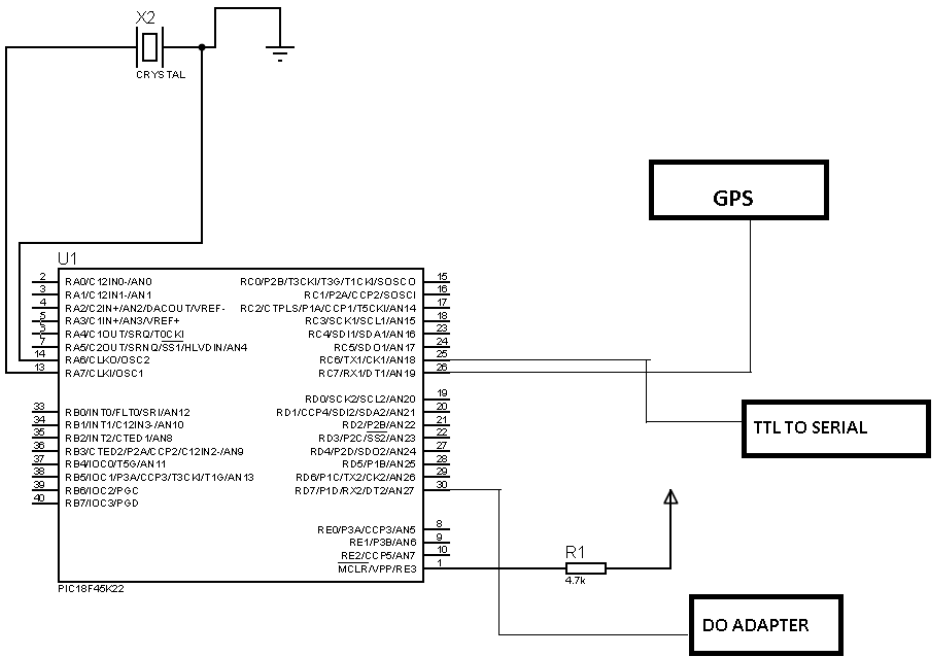

Fig. B-3. The circuit diagram for the PIC microcontroller and a single DO sensor aboard the sensor platform.

The ground station comprises a laptop computer with a customized LabVIEW interface (National Instruments, Austin, TX, USA) that allows for user-input for navigation and data logging (Fig. B-4). In manual navigation mode, the user interface (UI) logs coordinate data from the USV in a text file, and displays the path of the vehicle in a graphical interface. In automated mode, the user additionally is able to enter a target set of coordinates for the USV to move towards. Currently, if a user wants to enter another target coordinate, they can enter another set of coordinates through the UI once the USV is within a customizable distance to the target location. Future work will be completed to allow a user to enter multiple points right away and have the USV move through the listed locations automatically.

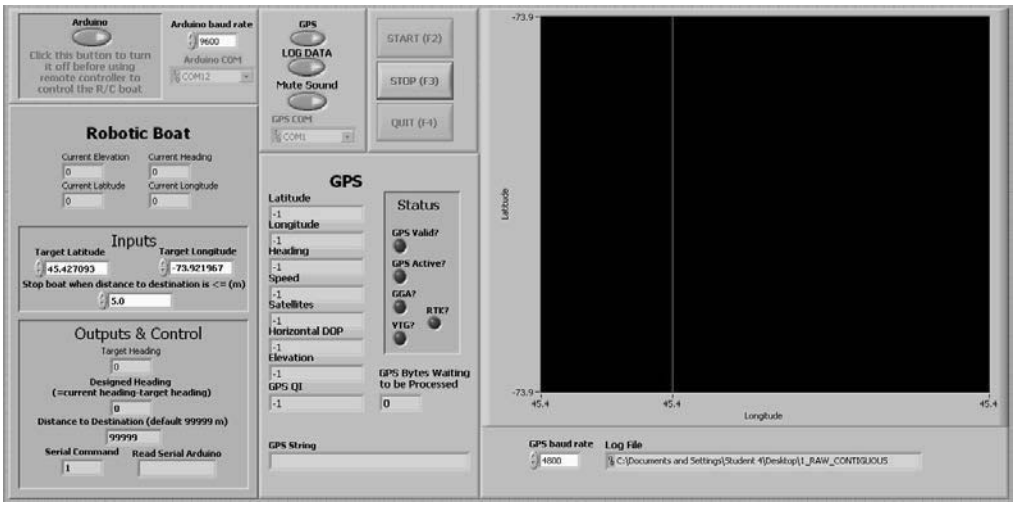

Fig. B-4. The front panel of a LabVIEW user interface for automated navigation and data collection

C. AST range test

One strength of a low-cost USV that can carry diverse sensor payloads is that it can be used to test various water quality instruments and sensors. The USV presented here was used to test a temperature and depth sensor based on an Acoustic Sensory Telemetry (AST) system.

AST systems are the combination of water quality sensors and acoustic telemetric tags for the measurement of water quality contaminants. Acoustic telemetric tags are a common method of studying the movement, location, and behavior of underwater organisms – the tags are typically attached to an organism and send data to a submerged receiver via supersonic acoustic pulses (Fig. C-1). With the addition of sensors, the tags provide a unique way in which to conduct *in-situ* measurements and monitoring of the physico-chemical properties of water. Currently, there are only temperature and depth sensors on the market, but new sensors are being designed to measure pH, DO, various heavy metals and nutrients, and even organic compounds. Due to the small size of the sensors and capacity for *in-situ* measurements, these tags have potential applications for wide-scale monitoring non-point source pollution and various contaminants, and can be deployed attached to an organism or a USV.

Three tags of different sizes were tested on land (Table C-1) and in water (Table C-2). The range was significantly reduced on land, as supersonic frequency acoustic waves can be highly distorted out of water. The range for the three tags when tested underwater increased with tag size due to increased power available in larger tags.

Table C-1. Communication range for AST tags out of water.

AST tag	range (m)
V7 (A69-1601-31512)	0.06
V8 (A69-1601-31513)	0.22
V16 (A69-9001-27179)	0.60

Table C-2. Communication range for AST tags in water.

AST tag	range (m)
V7 (A69-1601-31512)	63
V8 (A69-1601-31513)	149
V16 (A69-9001-27179)	170

Fig. C-1. The V16 coded tag provided by Vemco for acoustic sensory telemetry testing.